

Ballistic Convergence in Hit-and-Run Monte Carlo and a Coordinate-free Randomized Kaczmarz Algorithm

Nawaf Bou-Rabee*

Andreas Eberle[†]Stefan Oberdörster[‡]

December 2024

Abstract

Hit-and-Run is a coordinate-free Gibbs sampler, yet the quantitative advantages of its coordinate-free property remain largely unexplored beyond empirical studies. In this paper, we prove sharp estimates for the Wasserstein contraction of Hit-and-Run in Gaussian target measures via coupling methods and conclude mixing time bounds. Our results uncover ballistic and superdiffusive convergence rates in certain settings. Furthermore, we extend these insights to a coordinate-free variant of the randomized Kaczmarz algorithm, an iterative method for linear systems, and demonstrate analogous convergence rates. These findings offer new insights into the advantages and limitations of coordinate-free methods for both sampling and optimization.


1 Introduction


The Gibbs sampler, also known as Glauber dynamics or the heat-bath algorithm, is a Markov chain Monte Carlo method for sampling from complex multivariate distributions by alternately sampling from each variate’s one-dimensional conditional distribution. This approach reduces the high-dimensional sampling problem to dimension one; for overviews, see [7, 29]. The method was introduced by Glauber [16] for simulations of Ising models, and later introduced to statistics by Geman and Geman [15] in the context of image processing. Gelfand and Smith [14] further popularized it for Bayesian inference, and today, the Gibbs sampler is widely available in probabilistic programming languages such as BUGS [35], JAGS [30], and Nimble [12].

The Gibbs sampler relies on a chosen coordinate system. When the coordinate directions are not aligned with the geometry of the target distribution – particularly when the components are highly correlated – the sampler may exhibit diffusive behavior, slowing convergence. For example, in a centered bivariate normal with unit variances and correlation coefficient $\rho \in (-1, 1)$, the systematic-scan Gibbs sampler at a current state (x, y) , generates a Markov chain with updates

$$X \sim \mathcal{N}(\rho y, 1 - \rho^2), \quad \text{and} \quad Y \sim \mathcal{N}(\rho X, 1 - \rho^2).$$

*Department of Mathematical Sciences, Rutgers University, nawaf.bourabee@rutgers.edu 

[†]Institute for Applied Mathematics, University of Bonn, eberle@uni-bonn.de 

[‡]Institute for Applied Mathematics, University of Bonn, oberdoerster@uni-bonn.de 

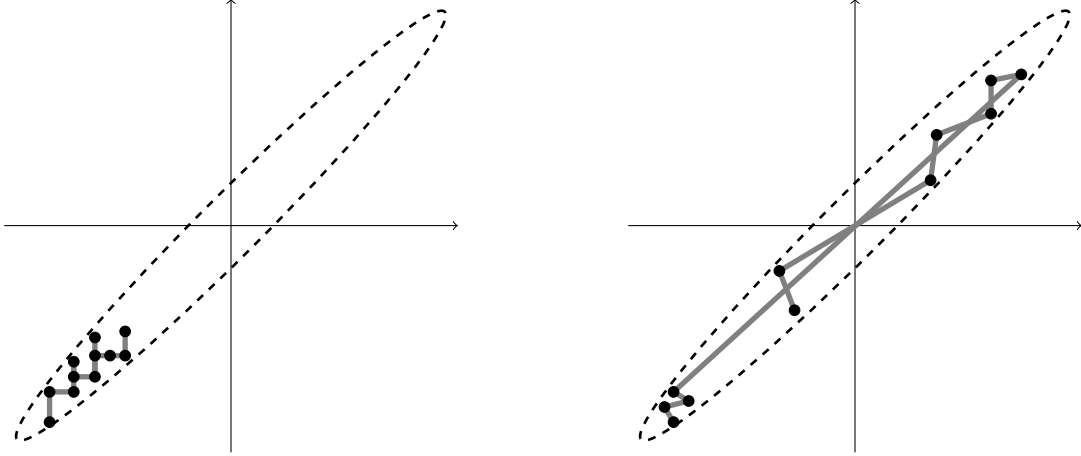


Figure 1: Comparison of 10 steps of Gibbs vs. Hit-and-Run in a narrow bivariate Gaussian target with condition number $\kappa \gg 1$: Gibbs is limited to small, incremental steps along the coordinate axes, resulting in a slow diffusive mixing rate of κ^{-1} . In contrast, Hit-and-Run samples directions uniformly and can take large, global steps whenever its sampled direction sufficiently aligns with the major axis of the ellipse. This enables Hit-and-Run to achieve a faster ballistic mixing rate of $\kappa^{-1/2}$ (see Section 3.3).

If we consider only the evolution of the Y -component and define $h = 1 - \rho^2$, the discrete generator of this component converges to that of an Ornstein-Uhlenbeck process in the high-correlation limit, specifically: for any $y \in \mathbb{R}$ and twice continuously differentiable function $f : \mathbb{R} \rightarrow \mathbb{R}$,

$$\lim_{h \searrow 0} \frac{\mathbb{E}f(Y) - f(y)}{h} = -yf'(y) + f''(y).$$

This diffusive behavior of Gibbs is illustrated in the left panel of Figure 1.

The Gibbs sampler’s reliance on a specific coordinate system motivates Hit-and-Run, a coordinate-free alternative. Hit-and-Run samples from the target “conditioned” to a line through the current state chosen uniformly at random. As described by Andersen and Diaconis [1], the algorithm “hits” a uniformly distributed direction and then “runs” within that direction from the current state. The basic Hit-and-Run method for sampling from an arbitrary probability density in high-dimensional Euclidean space was first introduced by Turchin [37], and later by Smith [34] for sampling from the uniform distribution over a convex body.

Hit-and-Run is a well-studied method for uniform sampling over convex bodies [23, 25, 38, 24]. Lovász [23] used conductance arguments to prove a sharp diffusive mixing time bound for Hit-and-Run, showing that it scales linearly with the condition number of the body, under the assumption of a warm start. Later, Lovász and Vempala [24] removed the warm start assumption by adding a warm-up phase [25].

In contrast, the ball walk [21], while simpler to implement, can require exponential time to escape corners, making it less practical for general convex bodies. The recently proposed In-and-Out sampler [22], a proximal sampler for uniform distributions over convex bodies, achieves similar runtime complexity to the ball walk but offers stronger guarantees in terms of Rényi divergence.

Appendix A of [22] provides a detailed comparison of the ball walk, Hit-and-Run methods, and related methods for uniform sampling over convex bodies.

Chen and Eldan [10] improved upon Lovász’s bounds for Hit-and-Run in isotropic bodies by using stochastic localization [11], replacing the dependence on the condition number with a dependence on the KLS constant. More recently, Ascolani, Lavenant and Zanella [2] showed relative entropy contraction at a diffusive rate for both Gibbs and Hit-and-Run in strongly log-concave distributions, a setting that generalizes uniform sampling over convex bodies.

Hit-and-Run has inspired numerous variations and generalizations over the years [9, 3, 1]. Andersen and Diaconis [1] introduced a significant generalization of Hit-and-Run that unifies a wide range of methods, including the Gibbs sampler, Swendsen-Wang algorithm, data augmentation, auxiliary variable Markov chains [33], slice sampling, and the Burnside process. This framework allows the next state to be sampled from an abstract line through the current state, where the direction is drawn from a generalized distribution that need not be uniform. Recently, this framework has been extended to include locally adaptive Hamiltonian Monte Carlo methods, such as the No-U-Turn Sampler [4].

Main result for Hit-and-Run Unlike the Gibbs sampler, which is constrained to moving along the coordinate axes, Hit-and-Run can move in any direction. This key distinction allows Hit-and-Run to make *global moves*, even when Gibbs is restricted to local ones. Figure 1 illustrates this advantage, which has been empirically observed in bivariate Gaussians [9], but has not yet been rigorously quantified. A key contribution of this paper is to provide a rigorous quantification of this advantage of coordinate-free Monte Carlo methods and to show its limitations.

We focus on centered Gaussian target measures with covariance matrix \mathcal{C} . This setting is not trivial because, even for Gaussian targets, the transition distribution of Hit-and-Run is not Gaussian, see Figure 6. In this context, we state our results for the broader class of *generalized Hit-and-Run samplers*, which allows directions to be chosen from an arbitrary distribution τ on the unit sphere, rather than just the uniform distribution.

To obtain a mixing time upper bound, we use a coupling argument. Specifically, we consider a synchronous coupling of two copies of the generalized Hit-and-Run sampler starting from different initial points. Remarkably, at each step, the difference between the components of this coupling is projected onto a random $(d - 1)$ -dimensional linear subspace. This insight allows us to apply a simple yet powerful contraction estimate for such random projections formalized in Lemma 1.

Our analysis leads to sharp estimates on the Wasserstein contraction of the generalized Hit-and-Run sampler guaranteeing a rate given by

$$\rho = \frac{1}{2} \inf_{|\zeta|=1} \mathbb{E}_{v \sim \tau} \left(\zeta \cdot \frac{\mathcal{C}^{-1/2}v}{|\mathcal{C}^{-1/2}v|} \right)^2$$

which, when combined with a one-step overlap bound, yields a bound on the total variation mixing time. Importantly, our coupling-based approach does not require the initial distribution to be warm.

d	\mathcal{C}	$\rho \asymp$	Speed of Mixing
2	$\text{diag}(\kappa, 1)$	$\kappa^{-1/2}$	ballistic
3	$\text{diag}(\kappa, \kappa, 1)$	$\kappa^{-1/2}$	ballistic
3	$\text{diag}(\kappa, 1, 1)$	$\kappa^{-1} \log \kappa$	superdiffusive
4	$\text{diag}(\kappa, 1, 1, 1)$	κ^{-1}	diffusive

Table 1: *Mixing speed and Wasserstein contraction rate ρ for Hit-and-Run for low-dimensional Gaussian target measures $\mathcal{N}(0, \mathcal{C})$ with varying combinations of low ($\kappa^{-1} \ll 1$) and high modes with respect to \mathcal{C}^{-1} , see Section 3.3. The resulting mixing time bounds are of order ρ^{-1} , up to logarithmic factors. The symbol \asymp indicates quantities of the same order, see (19). Note that these bounds hold for any rotation of the given Gaussians, reflecting Hit-and-Run’s invariance under rotations. In particular, the first row quantifies the ballistic mixing of Hit-and-Run illustrated in Figure 1.*

Table 1 summarizes the resulting rates for Hit-and-Run, i.e., $\tau = \text{Unif}(\mathbb{S}^{d-1})$, in various low-dimensional cases. Notably, our results rigorously explain the empirically observed ballistic speed-up in dimension two [9]. Beyond the bivariate case, we show that this speed-up occurs only if the number of high modes with respect to \mathcal{C}^{-1} is sufficiently small relative to the number of low modes.

Main result for coordinate-free randomized Kaczmarz Furthermore, we extend our findings on coordinate-free Monte Carlo methods to analogous optimization methods by examining the randomized Kaczmarz algorithm [36]. While the analogy between Monte Carlo and optimization methods is well established in the context of Gibbs samplers [32], it is less well-known for Hit-and-Run. Moreover, the advantages of coordinate-free approaches, to our knowledge, has not been rigorously quantified. Remarkably, the general contraction lemma for random projections formalized in Lemma 1, naturally applies to the convergence analysis of these methods.

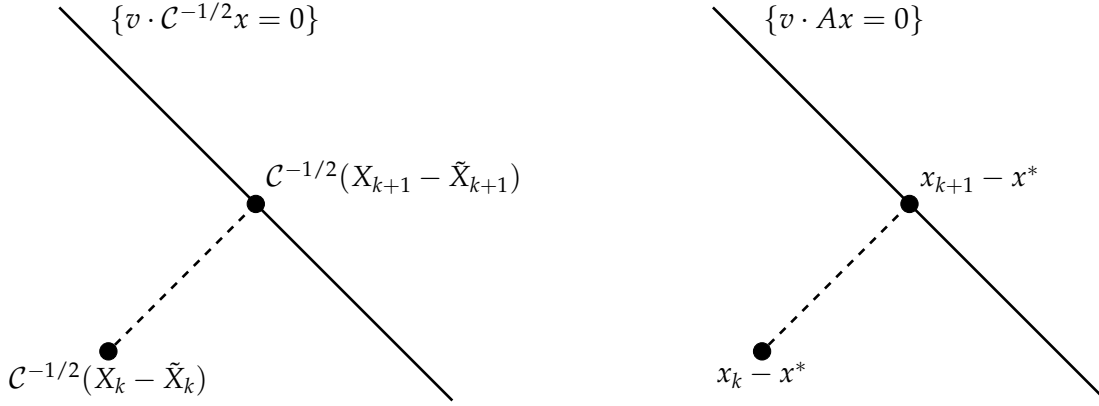
The randomized Kaczmarz algorithm is an iterative method for approximately solving overdetermined linear systems $Ax = b$. It works by iteratively projecting onto solution hyperplanes $\{e_i \cdot (Ax - b) = 0\}$ of randomly chosen equations from the system, where e_i denotes the i -th canonical basis vector. This algorithm is by construction restricted to the coordinate directions defined by the canonical basis of \mathbb{R}^d , making it analogous to random-scan Gibbs samplers.

Motivated by this restriction to particular coordinate directions, we introduce a *coordinate-free randomized Kaczmarz algorithm* which projects onto solution hyperplanes

$$\{v \cdot (Ax - b) = 0\}, \quad v \sim \text{Unif}(\mathbb{S}^{d-1}),$$

which are random linear combinations of the system’s equations. Extending this further, we consider the more general class of *generalized randomized Kaczmarz algorithms*, which allow for an arbitrary distribution τ on the unit sphere. For this generalization, we prove that the mean error decays at the rate

$$\rho = \frac{1}{2} \inf_{|\zeta|=1} \mathbb{E}_{v \sim \tau} \left(\zeta \cdot \frac{A^T v}{|A^T v|} \right)^2.$$



(a) Difference between components of a synchronous coupling of two copies of Hit-and-Run Monte Carlo. (b) Difference between coordinate-free randomized Kaczmarz and the solution x^* of the linear system.

Figure 2: Random projections onto hyperplanes (solid lines) defined using $v \sim \text{Unif}(\mathbb{S}^{d-1})$.

This result follows from applying Lemma 1, by interpreting the error as the difference between two copies, one of which is at the solution. In each iteration, the difference is projected onto a random $(d - 1)$ -dimensional linear subspace, enabling the application of the general contraction lemma for random projections given below. As a special case, our result recovers the diffusive convergence rate established in [36] for the coordinate-bound variant. Moreover, the ideas developed for Hit-and-Run transfer seamlessly to the randomized Kaczmarz algorithm, revealing the potential for a diffusive-to-ballistic speed-up in its coordinate-free variant.

General contraction lemma for random projections We now state and prove a central lemma that quantifies the average contraction resulting from random projections onto $(d - 1)$ -dimensional linear subspaces of \mathbb{R}^d . This lemma plays a crucial role in the convergence analyses of both Hit-and-Run and coordinate-free randomized Kaczmarz, as illustrated in Figure 2.

Lemma 1. Let η be a probability measure on \mathbb{R}^d . For $w \sim \eta$, define the random projection

$$\Pi_w = I_d - \frac{w \otimes w}{|w|^2}$$

which projects any vector onto the orthogonal complement of $\text{span}(w)$. For all $z \in \mathbb{R}^d$, Π_w satisfies

$$\mathbb{E}_{w \sim \eta} |\Pi_w z|^2 \leq \left(1 - \inf_{|\zeta|=1} \mathbb{E}_{w \sim \eta} \left(\zeta \cdot \frac{w}{|w|}\right)^2\right) |z|^2. \quad (1)$$

The expectation on the right-hand side of (1) measures the average contraction rate of a fixed vector z under the random projection Π_w for $w \sim \eta$. Taking the infimum over all unit vectors ζ yields a global rate of average contraction for the random projection.

Proof of Lemma 1. Let $z \in \mathbb{R}^d$. For all unit vectors $w \in \mathbb{R}^d$, it holds

$$|\Pi_w z|^2 = |z - (z \cdot w)w|^2 = \left(1 - \left(\frac{z}{|z|} \cdot w\right)^2\right) |z|^2.$$

Using this, we can compute

$$\mathbb{E}_{w \sim \eta} |\Pi_w z|^2 = \mathbb{E}_{w \sim \eta} |\Pi_{w/|w|} z|^2 \leq \left(1 - \inf_{|\zeta|=1} \mathbb{E}_{w \sim \eta} \left(\zeta \cdot \frac{w}{|w|}\right)^2\right) |z|^2.$$

This completes the proof. \square

Organization of paper The remainder of the paper is organized as follows. Section 2 introduces a generalized Hit-and-Run sampler, encompassing Hit-and-Run as a special case. Sections 3.1 and 3.2 provide upper and lower bounds, respectively, on the Wasserstein contraction rate for this class of methods when applied to Gaussian target measures. Section 3.3 discusses the rates achieved by Hit-and-Run. Section 3.4 combines the Wasserstein contraction results with a one-step overlap bound from Section 3.5 to obtain mixing time upper bounds for Hit-and-Run. Finally, Section 4 extends these techniques to analyze the generalized randomized Kaczmarz algorithm.

Acknowledgements

We wish to acknowledge Ahmed Bou-Rabee, Bob Carpenter, Francis Lörler, and Andre Wibosono for useful discussions. N. Bou-Rabee was partially supported by NSF grant No. DMS-2111224. A. Eberle and S. Oberdörster were supported by the Deutsche Forschungsgemeinschaft (DFG, German Research Foundation) under Germany's Excellence Strategy – EXC-2047/1 – 390685813.

2 The generalized Hit-and-Run sampler

In this section, we present a rigorous definition of the Hit-and-Run transition kernel and subsequently extend it by allowing for arbitrary distributions of the directions.

Let μ be an absolutely continuous target probability measure on \mathbb{R}^d with density with respect to Lebesgue measure also denoted by $\mu(x)$, $x \in \mathbb{R}^d$. To describe the Hit-and-Run transition step rigorously, let \mathbb{S}^{d-1} denote the unit sphere in \mathbb{R}^d , and define the line through $x \in \mathbb{R}^d$ in the direction $v \in \mathbb{S}^{d-1}$ as

$$L(x, v) = \{x + hv \mid h \in \mathbb{R}\}.$$

It corresponds to the image of the displacement map $\Delta_{x,v} : \mathbb{R} \rightarrow \mathbb{R}^d$, $\Delta_{x,v}(h) = x + hv$ which maps a scalar displacement h to the corresponding point on the line. Once a parametrization of the line is fixed, a regular version of the conditional distribution of μ given $L(x, v)$ is the push forward

$$\mu(\cdot | L(x, v)) = \mu_{x,v} \circ \Delta_{x,v}^{-1}$$

of the one-dimensional displacement measure $\mu_{x,v}$ on \mathbb{R} defined via its almost everywhere finite density

$$\mu_{x,v}(h) \propto \mu(x + hv). \quad (2)$$

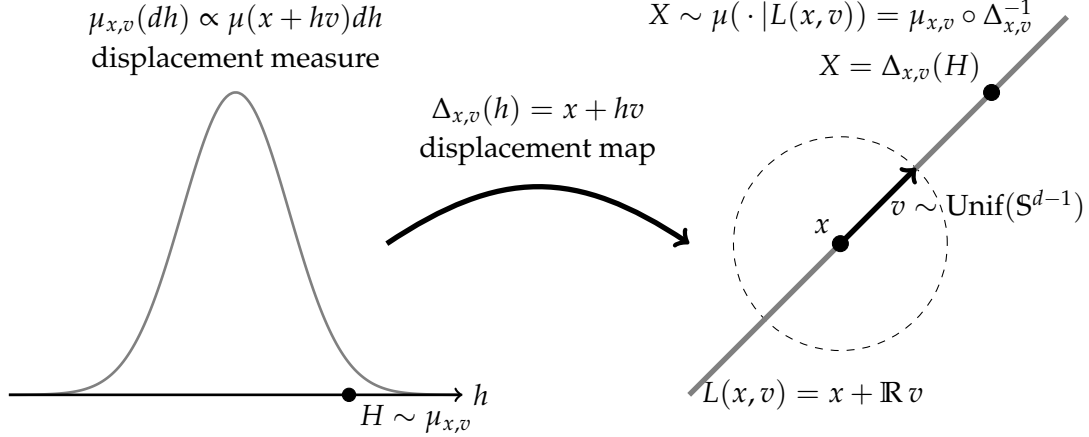


Figure 3: Transition step of Hit-and-Run from current state x to next state X .

A transition of Hit-and-Run proceeds as follows: Given the current state $x \in \mathbb{R}^d$, the direction $v \sim \text{Unif}(\mathbb{S}^{d-1})$ defines a line through x drawn uniformly at random. The next state $X \sim \mu(\cdot | L(x, v))$ is realized as $X = \Delta_{x,v}(H) = x + Hv$ with a random displacement $H \sim \mu_{x,v}$. See Figure 3.

Note that the line $L(x, v)$ and correspondingly the distribution $\mu(\cdot | L(x, v))$ do not depend on the specific choice of anchor point x on the line while the displacement map $\Delta_{x,v}$ and measure $\mu_{x,v}$ do.

Algorithm 1. Hit-and-Run $X \sim \pi_{\text{H\&R}}(x, \cdot)$

(Hit Step) Sample a direction $v \sim \text{Unif}(\mathbb{S}^{d-1})$.

(Run Step) Sample a scalar displacement $H \sim \mu_{x,v}$.

(Output) Return $X = x + Hv$.

Let $\sigma_{d-1} = \text{Unif}(\mathbb{S}^{d-1})$ be the normalized Haar measure on \mathbb{S}^{d-1} . The transition kernel of Hit-and-Run is given by

$$\pi_{\text{H\&R}}(x, A) = \int_{\mathbb{S}^{d-1}} \int_{\mathbb{R}} 1_A(x + hv) \mu_{x,v}(dh) \sigma_{d-1}(dv) \quad (3)$$

for $x \in \mathbb{R}^d$ and measurable sets $A \subset \mathbb{R}^d$. Changing from spherical to Cartesian coordinates yields the equivalent representation

$$\pi_{\text{H\&R}}(x, dy) = 1_{\{y \neq x\}} \frac{2}{a_{d-1}} \frac{1}{|y - x|^{d-1}} \mu_{x, \frac{y-x}{|y-x|}}(|y - x|) dy \quad (4)$$

where a_{d-1} denotes the surface area of \mathbb{S}^{d-1} . Similar representations appear in [9, 10]. This representation will be used to quantify the overlap between the transition distributions of two copies of Hit-and-Run starting at different points, see Lemma 4.

By allowing for more general probability distributions τ on \mathbb{S}^{d-1} in the *Hit Step*, we can define the generalized Hit-and-Run sampler with transition kernel

$$\pi_{\text{gH\&R}}(x, A) = \int_{\mathbb{S}^{d-1}} \int_{\mathbb{R}} 1_A(x + hv) \mu_{x,v}(dh) \tau(dv). \quad (5)$$

This generalized Hit-and-Run sampler encompasses not only Hit-and-Run for $\tau = \text{Unif}(\mathbb{S}^{d-1})$, but also the random-scan Gibbs sampler corresponding to $\tau = \frac{1}{d} \sum_{i=1}^d \delta_{e_i}$ where $\{e_i\}_{1 \leq i \leq d}$ is the canonical basis of \mathbb{R}^d . In the latter case, τ equals the uniform distribution over the d coordinate directions. The next theorem ensures reversibility of this general class of samplers with respect to the target distribution.

Theorem 1. *The transition kernel $\pi_{\text{gH\&R}}$ of generalized Hit-and-Run is reversible with respect to μ .*

Proof. Since $\mu_{x,v}(dh) = \frac{\mu(x+hv)}{\int_{\mathbb{R}} \mu(x+sv) ds} dh$ for all $x, v \in \mathbb{R}^d$ by (2), inserting (3) and changing variables twice shows for any measurable sets $A, B \subset \mathbb{R}^d$,

$$\begin{aligned}
\int_A \pi_{\text{gH\&R}}(x, B) \mu(dx) &= \int_{\mathbb{R}^d} \int_{\mathbb{S}^{d-1}} \int_{\mathbb{R}} 1_A(x) 1_B(x+hv) \mu_{x,v}(dh) \tau(dv) \mu(dx) \\
&= \int_{\mathbb{R}^d} \int_{\mathbb{S}^{d-1}} \int_{\mathbb{R}} 1_A(x) 1_B(x+hv) \frac{\mu(x) \mu(x+hv)}{\int_{\mathbb{R}} \mu(x+sv) ds} dh \tau(dv) dx \\
&= \int_{\mathbb{R}^d} \int_{\mathbb{S}^{d-1}} \int_{\mathbb{R}} 1_A(x-hv) 1_B(x) \frac{\mu(x-hv) \mu(x)}{\int_{\mathbb{R}} \mu(x+sv) ds} dh \tau(dv) dx \\
&= \int_{\mathbb{R}^d} \int_{\mathbb{S}^{d-1}} \int_{\mathbb{R}} 1_A(x+hv) 1_B(x) \frac{\mu(x+hv) \mu(x)}{\int_{\mathbb{R}} \mu(x+sv) ds} dh \tau(dv) dx \\
&= \int_{\mathbb{R}^d} \int_{\mathbb{S}^{d-1}} \int_{\mathbb{R}} 1_A(x+hv) 1_B(x) \mu_{x,v}(dh) \tau(dv) \mu(dx) \\
&= \int_B \pi_{\text{gH\&R}}(x, A) \mu(dx).
\end{aligned}$$

Thus, the kernel $\pi_{\text{gH\&R}}$ is reversible with respect to μ . □

3 Generalized Hit-and-Run in Gaussian distributions

Consider the centered Gaussian target measure

$$\gamma^{\mathcal{C}} = \mathcal{N}(0, \mathcal{C}) \quad \text{on } \mathbb{R}^d.$$

Given a line $L(x, v)$, the corresponding scalar displacement measure, as defined in (2), is characterized by its density

$$\gamma_{x,v}^{\mathcal{C}}(h) \propto \gamma^{\mathcal{C}}(x+hv) \propto e^{-\frac{1}{2} | \mathcal{C}^{-1/2} v |^2 h^2 - x \cdot \mathcal{C}^{-1} v h} \propto \exp\left(-\frac{| \mathcal{C}^{-1/2} v |^2}{2} \left(h + \frac{x \cdot \mathcal{C}^{-1} v}{| \mathcal{C}^{-1/2} v |^2}\right)^2\right).$$

Thus,

$$\gamma_{x,v}^{\mathcal{C}} = \mathcal{N}\left(-\frac{x \cdot \mathcal{C}^{-1} v}{| \mathcal{C}^{-1/2} v |^2}, | \mathcal{C}^{-1/2} v |^{-2}\right). \quad (6)$$

For $Z \sim \mathcal{N}(0, 1)$, the random variable

$$H = -\frac{x \cdot \mathcal{C}^{-1} v}{| \mathcal{C}^{-1/2} v |^2} + \frac{Z}{| \mathcal{C}^{-1/2} v |} \quad \text{satisfies} \quad H \sim \gamma_{x,v}^{\mathcal{C}}. \quad (7)$$

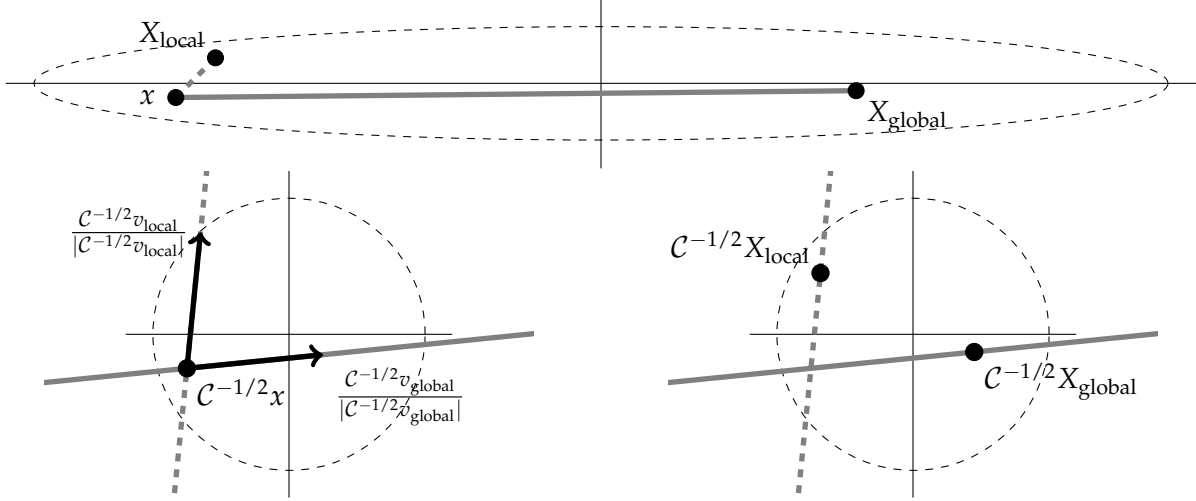


Figure 4: Two realizations of a Hit-and-Run transition starting from x with $C = \text{diag}(\kappa, 1)$, $\kappa > 1$, see (8). The directions v_{local} and v_{global} result in vastly different moves. The distribution $\text{Law}(C^{-1/2}v/|C^{-1/2}v|)$, for $v \sim \text{Unif}(\mathbb{S}^1)$, favors directions that lead to local moves. However, the probability of making a global move is of order $\kappa^{-1/2}$, see Figure 5, allowing Hit-and-Run to achieve ballistic mixing, as discussed in Section 3.3.

With $v \sim \tau$ independent of Z , a transition step $X \sim \pi_{\text{gH\&R}}(x, \cdot)$ of generalized Hit-and-Run with invariant measure γ^C satisfies

$$\begin{aligned} C^{-1/2}X &= C^{-1/2}(x + Hv) = \left(I_d - \frac{C^{-1/2}v \otimes C^{-1/2}v}{|C^{-1/2}v|^2}\right)C^{-1/2}x + Z \frac{C^{-1/2}v}{|C^{-1/2}v|} \\ &= \Pi_{C^{-1/2}v} C^{-1/2}x + Z \frac{C^{-1/2}v}{|C^{-1/2}v|} \end{aligned} \quad (8)$$

where $\Pi_w = I_d - |w|^{-2}w \otimes w$, $w \in \mathbb{R}^d$ is the projection onto the orthogonal complement of $\text{span}(w)$, as defined in Lemma 1.

In the natural coordinates $C^{-1/2}x$, the target measure turns into the canonical Gaussian measure. Generalized Hit-and-Run then replaces the component of $C^{-1/2}x$ in the random direction $C^{-1/2}v/|C^{-1/2}v|$ by a sample from the canonical Gaussian. Note that even in the case of Hit-and-Run, the distribution of $C^{-1/2}v/|C^{-1/2}v|$ is not uniform, unlike the distribution of v . This is illustrated in Figure 5. The transition via the natural coordinates is depicted in Figure 4.

3.1 Wasserstein contraction of generalized Hit-and-Run: Lower bound

In the natural coordinates $C^{-1/2}x$, the transition step consists of two distinct operations: a projection that removes the current state's component in direction $C^{-1/2}v$, and a complete randomization of the component using a standard Gaussian random variable Z , see (8). Importantly, the auxiliary random variables v and Z are independent of the current state x .

By synchronously coupling the auxiliary random variables in two copies of generalized Hit-and-Run, the transition of their difference reduces to a projection onto a random $(d - 1)$ -dimensional

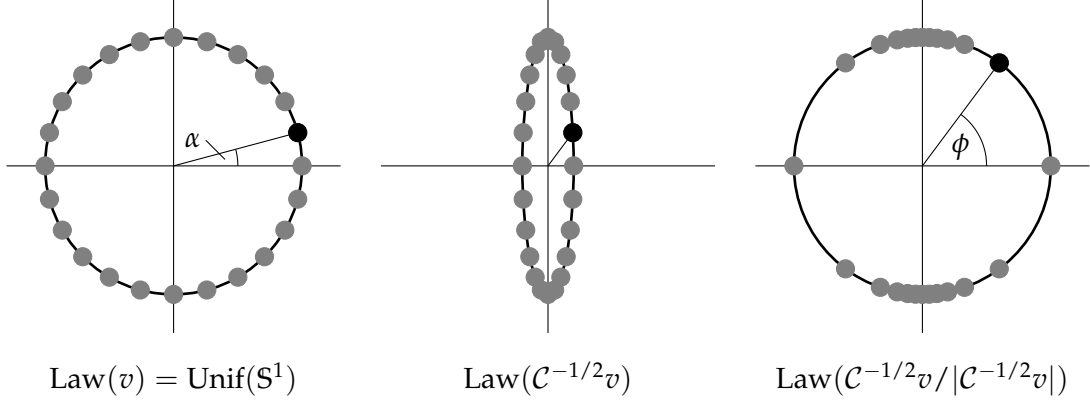


Figure 5: Transformation of $\text{Law}(v) = \text{Unif}(S^1)$ used in Hit-and-Run under the change-of-coordinates $x \mapsto C^{-1/2}x$ in the bivariate case with $C = \text{diag}(\kappa, 1)$, $\kappa > 1$. The gray beads illustrate the redistribution of probability mass, which favors directions aligned with the high mode of C^{-1} . By elementary trigonometry, the angles α and $\phi(\alpha)$ in the original and transformed coordinates corresponding to the black bead are related by $\tan \phi(\alpha) = \kappa^{1/2} \tan \alpha$. Hence, for fixed $\phi(\alpha)$ we have $\alpha \asymp \kappa^{-1/2}$, see (19).

subspace:

$$C^{-1/2}(X - \tilde{X}) = \Pi_{C^{-1/2}v} C^{-1/2}(x - \tilde{x}) \quad (9)$$

where $x, \tilde{x} \in \mathbb{R}^d$, $X \sim \pi_{\text{gH\&R}}(x, \cdot)$, $\tilde{X} \sim \pi_{\text{gH\&R}}(\tilde{x}, \cdot)$ using the same $v \sim \tau$ and $Z \sim \mathcal{N}(0, 1)$. The law of $C^{-1/2}v$ determines the contraction properties of this coupling, as quantified in the next lemma using the L^2 -Wasserstein distance $\mathcal{W}_{C^{-1/2}}^2$ with respect to the metric induced by $|x|_{C^{-1/2}} = |C^{-1/2}x|$.

Lemma 2. *It holds*

$$\mathcal{W}_{C^{-1/2}}^2(\pi_{\text{gH\&R}}(x, \cdot), \pi_{\text{gH\&R}}(\tilde{x}, \cdot)) \leq (1 - \rho)|x - \tilde{x}|_{C^{-1/2}} \quad \text{for all } x, \tilde{x} \in \mathbb{R}^d \quad (10)$$

with

$$\rho = \frac{1}{2} \inf_{|\zeta|=1} \mathbb{E}_{v \sim \tau} \left(\zeta \cdot \frac{C^{-1/2}v}{|C^{-1/2}v|} \right)^2. \quad (11)$$

The lemma provides a lower bound for the global Wasserstein contraction rate of generalized Hit-and-Run, defined as the supremum over all ρ satisfying (10). This lower bound is sharp in the sense that any $\rho' > 0$ such that (10) holds with ρ' instead of ρ , satisfies $\rho' \leq 3\rho$, see Lemma 3 below.

A lower bound for the global Wasserstein contraction rate implies a lower bound for the coarse Ricci curvature of $(\mathbb{R}^d, |\cdot|_{C^{-1/2}})$ equipped with generalized Hit-and-Run which has far-reaching consequences [28, 19].

If τ is symmetric with respect to reflection through the origin, i.e., $\tau(A) = \tau(-A)$ for all measurable $A \subset S^{d-1}$, then $\text{Law}(C^{-1/2}v/|C^{-1/2}v|)$ inherits this symmetry. In this case, the contraction rate can be expressed as

$$\rho = \frac{1}{2} \inf_{|\zeta|=1} \text{Var}_{v \sim \tau} \left(\zeta \cdot \frac{C^{-1/2}v}{|C^{-1/2}v|} \right). \quad (12)$$

Proof of Lemma 2. The proof uses Lemma 1, the general contraction lemma for random projections. Let $z = \mathcal{C}^{-1/2}(x - \tilde{x})$ and consider a synchronous coupling (X, \tilde{X}) of $\pi_{\text{gH\&R}}(x, \cdot)$ and $\pi_{\text{gH\&R}}(\tilde{x}, \cdot)$. From (9),

$$|X - \tilde{X}|_{\mathcal{C}^{-1/2}} = |\mathcal{C}^{-1/2}(\tilde{X} - X)| = |\Pi_{\mathcal{C}^{-1/2}v} z|$$

so that by Lemma 1,

$$\begin{aligned} \mathcal{W}_{\mathcal{C}^{-1/2}}^2(\pi_{\text{gH\&R}}(x, \cdot), \pi_{\text{gH\&R}}(\tilde{x}, \cdot)) &\leq \sqrt{\mathbb{E}_{v \sim \tau} |X - \tilde{X}|_{\mathcal{C}^{-1/2}}^2} = \sqrt{\mathbb{E}_{v \sim \tau} |\Pi_{\mathcal{C}^{-1/2}v} z|^2} \\ &\leq \sqrt{1 - \inf_{|\zeta|=1} \mathbb{E}_{v \sim \tau} \left(\zeta \cdot \frac{\mathcal{C}^{-1/2}v}{|\mathcal{C}^{-1/2}v|} \right)^2} |z| \leq \left(1 - \frac{1}{2} \inf_{|\zeta|=1} \mathbb{E}_{v \sim \tau} \left(\zeta \cdot \frac{\mathcal{C}^{-1/2}v}{|\mathcal{C}^{-1/2}v|} \right)^2 \right) |x - \tilde{x}|_{\mathcal{C}^{-1/2}}. \end{aligned}$$

□

3.2 Wasserstein contraction of generalized Hit-and-Run: Upper bound

We now show the Wasserstein contraction rate obtained in Lemma 2 for generalized Hit-and-Run to be sharp up to a multiplicative constant. By (5), the averaging operator associated with generalized Hit-and-Run takes the form

$$\pi_{\text{gH\&R}} f(x) = \int_{S^{d-1}} \int_{\mathbb{R}} f(x + hv) \gamma_{x,v}^{\mathcal{C}}(dh) \tau(dv). \quad (13)$$

The spectral radius of this operator acting on the orthogonal complement of the constant functions in $L^2(\gamma^{\mathcal{C}})$ is

$$1 - \lambda = \sup_{f \perp 1, \|f\|_{L^2(\gamma^{\mathcal{C}})}=1} \|\pi_{\text{gH\&R}} f\|_{L^2(\gamma^{\mathcal{C}})}. \quad (14)$$

Lemma 3. *Let ρ be as defined in Lemma 2. It holds*

$$\lambda \leq 3\rho. \quad (15)$$

In particular, any $\rho' > 0$ such that

$$\mathcal{W}_{\mathcal{C}^{-1/2}}^2(\pi_{\text{gH\&R}}(x, \cdot), \pi_{\text{gH\&R}}(\tilde{x}, \cdot)) \leq (1 - \rho') |x - \tilde{x}|_{\mathcal{C}^{-1/2}} \quad \text{for all } x, \tilde{x} \in \mathbb{R}^d \quad (16)$$

satisfies

$$\rho' \leq 3\rho. \quad (17)$$

Note that $\rho \leq \lambda$, since the lower bound ρ on the coarse Ricci curvature of $(\mathbb{R}^d, |\cdot|_{\mathcal{C}^{-1/2}})$ equipped with the family of probability measures $(\pi_{\text{gH\&R}}(x, \cdot))_{x \in \mathbb{R}^d}$, implied by Lemma 2 and $\mathcal{W}^1 \leq \mathcal{W}^2$, yields $1 - \lambda \leq 1 - \rho$, see [8, 28]. Similarly, assertion (17) follows from (15) as any $\rho' > 0$ satisfying (16) provides a lower bound ρ' on the coarse Ricci curvature so that

$$1 - 3\rho \leq 1 - \lambda \leq 1 - \rho'$$

proving (17).

Proof. We are left to show (15). Define

$$f_\zeta(x) = \zeta \cdot \mathcal{C}^{-1/2}x \quad \text{for } |\zeta| = 1.$$

Since $f_\zeta \in L^2(\gamma^\mathcal{C})$ with $f_\zeta \perp 1$ and $\|f_\zeta\|_{L^2(\gamma^\mathcal{C})} = 1$, by (14),

$$1 - \lambda \geq \sup_{|\zeta|=1} \|\pi_{\text{gH\&R}} f_\zeta\|_{L^2(\gamma^\mathcal{C})}. \quad (18)$$

Inserting the definition of f_ζ into (13) and using linearity as well as (6) yields

$$\begin{aligned} \pi_{\text{gH\&R}} f_\zeta(x) &= f_\zeta(x) + \int_{\mathbb{S}^{d-1}} \int_{\mathbb{R}} h \gamma_{x,v}^\mathcal{C}(dh) f_\zeta(v) \tau(dv) \\ &= f_\zeta(x) - \int_{\mathbb{S}^{d-1}} \left(\frac{\mathcal{C}^{-1/2}v}{|\mathcal{C}^{-1/2}v|^2} \cdot \mathcal{C}^{-1/2}x \right) f_\zeta(v) \tau(dv). \end{aligned}$$

With Fubini's theorem and the fact that

$$\int_{\mathbb{R}^d} (a \cdot \mathcal{C}^{-1/2}x) (b \cdot \mathcal{C}^{-1/2}x) \gamma^\mathcal{C}(dx) = a \cdot b \quad \text{for all } a, b \in \mathbb{R}^d,$$

it then follows

$$\begin{aligned} \|\pi_{\text{gH\&R}} f_\zeta\|_{L^2(\gamma^\mathcal{C})}^2 &= \int_{\mathbb{R}^d} (\pi_{\text{gH\&R}} f_\zeta(x))^2 \gamma^\mathcal{C}(dx) \\ &= \|f_\zeta\|_{L^2(\gamma^\mathcal{C})}^2 - 2 \int_{\mathbb{S}^{d-1}} \int_{\mathbb{R}^d} f_\zeta(x) \left(\frac{\mathcal{C}^{-1/2}v}{|\mathcal{C}^{-1/2}v|^2} \cdot \mathcal{C}^{-1/2}x \right) \gamma^\mathcal{C}(dx) f_\zeta(v) \tau(dv) \\ &\quad + \int_{\mathbb{S}^{d-1}} \int_{\mathbb{S}^{d-1}} \int_{\mathbb{R}^d} \left(\frac{\mathcal{C}^{-1/2}v}{|\mathcal{C}^{-1/2}v|^2} \cdot \mathcal{C}^{-1/2}x \right) \left(\frac{\mathcal{C}^{-1/2}v'}{|\mathcal{C}^{-1/2}v'|^2} \cdot \mathcal{C}^{-1/2}x \right) \gamma^\mathcal{C}(dx) f_\zeta(v') \tau(dv') f_\zeta(v) \tau(dv) \\ &= 1 - 2 \int_{\mathbb{S}^{d-1}} \left(\zeta \cdot \frac{\mathcal{C}^{-1/2}v}{|\mathcal{C}^{-1/2}v|^2} \right) f_\zeta(v) \tau(dv) \\ &\quad + \int_{\mathbb{S}^{d-1}} \int_{\mathbb{S}^{d-1}} \left(\frac{\mathcal{C}^{-1/2}v}{|\mathcal{C}^{-1/2}v|^2} \cdot \frac{\mathcal{C}^{-1/2}v'}{|\mathcal{C}^{-1/2}v'|^2} \right) f_\zeta(v') \tau(dv') f_\zeta(v) \tau(dv) \\ &\geq 1 - 3 \int_{\mathbb{S}^{d-1}} \left(\zeta \cdot \frac{\mathcal{C}^{-1/2}v}{|\mathcal{C}^{-1/2}v|^2} \right)^2 \tau(dv) \end{aligned}$$

where in the last step we used the definition of f_ζ together with the triangle and Jensen's inequality

$$\begin{aligned} &\left| \int_{\mathbb{S}^{d-1}} \int_{\mathbb{S}^{d-1}} \left(\frac{\mathcal{C}^{-1/2}v}{|\mathcal{C}^{-1/2}v|^2} \cdot \frac{\mathcal{C}^{-1/2}v'}{|\mathcal{C}^{-1/2}v'|^2} \right) f_\zeta(v') \tau(dv') f_\zeta(v) \tau(dv) \right| \\ &\leq \int_{\mathbb{S}^{d-1}} \int_{\mathbb{S}^{d-1}} \frac{|f_\zeta(v')|}{|\mathcal{C}^{-1/2}v'|} \tau(dv') \frac{|f_\zeta(v)|}{|\mathcal{C}^{-1/2}v|} \tau(dv) = \left(\int_{\mathbb{S}^{d-1}} \left| \zeta \cdot \frac{\mathcal{C}^{-1/2}v}{|\mathcal{C}^{-1/2}v|} \right| \tau(dv) \right)^2 \\ &\leq \int_{\mathbb{S}^{d-1}} \left(\zeta \cdot \frac{\mathcal{C}^{-1/2}v}{|\mathcal{C}^{-1/2}v|} \right)^2 \tau(dv). \end{aligned}$$

By the elementary inequality $(1-x)^{1/2} \geq 1-x$ for $x \in [0, 1]$, then

$$\begin{aligned} \|\pi_{\text{gH\&R}} f_\zeta\|_{L^2(\gamma^\mathcal{C})} &\geq \left(1 - \min \left(1, 3 \int_{\mathbb{S}^{d-1}} \left(\zeta \cdot \frac{\mathcal{C}^{-1/2}v}{|\mathcal{C}^{-1/2}v|} \right)^2 \tau(dv) \right) \right)^{1/2} \\ &\geq 1 - 3 \int_{\mathbb{S}^{d-1}} \left(\zeta \cdot \frac{\mathcal{C}^{-1/2}v}{|\mathcal{C}^{-1/2}v|} \right)^2 \tau(dv). \end{aligned}$$

Inserting the last display into (18) yields

$$1 - \lambda \geq 1 - 3 \inf_{|\zeta|=1} \int_{\mathbb{S}^{d-1}} \left(\zeta \cdot \frac{\mathcal{C}^{-1/2}v}{|\mathcal{C}^{-1/2}v|} \right)^2 \tau(dv) = 1 - 3\rho$$

with ρ as defined in Lemma 2, showing (15). \square

3.3 Discussion of Wasserstein contraction of Hit-and-Run

In this section, we discuss the sharp contraction rates (11) resulting from Lemma 2 for Hit-and-Run, i.e., $\tau = \text{Unif}(\mathbb{S}^{d-1})$, in various Gaussian targets. By rotation and rescaling, we can assume \mathcal{C} to be a diagonal matrix with one mode having unit variance; e.g., in the bivariate case, we can take $\mathcal{C} = \text{diag}(\kappa, 1)$ where $\kappa \geq 1$ is the condition number of the corresponding Gaussian measure. The first four cases are summarized in Table 1.

We say that two expressions in κ are of the same order and denote

$$f(\kappa) \asymp g(\kappa) \quad \text{if and only if} \quad c g(\kappa') \leq f(\kappa') \leq C g(\kappa') \quad (19)$$

for constants $k, c, C > 0$ and all $\kappa' \geq k$. We further denote $x \propto y$ if $x = Cy$ for a constant $C > 0$.

Bivariate Case Consider $\mathcal{C} = \text{diag}(\kappa, 1)$, $\kappa \geq 1$. Since (12) holds for Hit-and-Run, among all unit vectors ζ , the smallest variance is achieved for $\zeta = e_1$, as illustrated in Figure 5. Thus, the contraction rate takes the form

$$\rho = \frac{1}{2} \mathbb{E}_{v \sim \sigma_1} \left(e_1 \cdot \frac{\mathcal{C}^{-1/2}v}{|\mathcal{C}^{-1/2}v|} \right)^2. \quad (20)$$

In particular, e_1 is the direction of least contraction on average under the random projection $\Pi_{\mathcal{C}^{-1/2}v}$.

Let $v(\alpha) = (\cos \alpha, \sin \alpha)$ and denote by $\phi(\alpha)$ the angle between e_1 and the transformed vector $\mathcal{C}^{-1/2}v(\alpha)/|\mathcal{C}^{-1/2}v(\alpha)|$, as illustrated in Figure 5. Then, due to the symmetry of the integral,

$$\rho = \frac{1}{2} \frac{2}{\pi} \int_0^{\pi/2} \left(e_1 \cdot \frac{\mathcal{C}^{-1/2}v(\alpha)}{|\mathcal{C}^{-1/2}v(\alpha)|} \right)^2 d\alpha = \frac{1}{\pi} \int_0^{\pi/2} \cos^2 \phi(\alpha) d\alpha.$$

Inserting $\phi(\alpha) = \arctan(\kappa^{1/2} \tan \alpha)$, the contraction rate evaluates to

$$\rho = \frac{1}{\pi} \int_0^{\pi/2} \frac{d\alpha}{\kappa \tan^2 \alpha + 1} = \frac{1}{2} (\kappa^{1/2} + 1)^{-1} \asymp \kappa^{-1/2}.$$

Thus, the contraction rate is of order $\kappa^{-1/2}$. This demonstrates that Hit-and-Run achieves ballistic contraction for bivariate Gaussian targets.

The contraction rate of Hit-and-Run can be understood geometrically as follows. For any fix $\phi(\alpha_{\text{global}}) \in (0, \pi/2)$, the directions in the general d -dimensional case can be partitioned into two sets:

$$\mathcal{V}_{\text{global}} = \{v \in \mathbb{S}^{d-1} : |\zeta \cdot v| \geq \cos \alpha_{\text{global}} \text{ for some } \zeta \in \mathcal{Z}\} \quad \text{and} \quad \mathcal{V}_{\text{local}} = \mathbb{S}^{d-1} \setminus \mathcal{V}_{\text{global}}$$

where $\mathcal{Z} \subset \mathbb{S}^{d-1}$ is the collection of directions achieving the infimum in (11).

In the bivariate case, $\mathcal{Z} = \{\pm e_1\}$ so that $\mathcal{V}_{\text{global}}$ consists of two polar-opposite spherical caps containing all directions within a α_{global} angle around $\pm e_1$. As $\phi(\alpha_{\text{global}})$ is fix, $\alpha_{\text{global}} \asymp \kappa^{-1/2}$, see Figure 5. These caps, as depicted in Figure 4, correspond to directions producing *global moves*, characterized by their ability to advance proportionally to the scale of the target distribution, or equivalently of constant order in the natural coordinates, in both modes.

The probability of choosing a direction in $\mathcal{V}_{\text{global}}$ is given by

$$\text{Unif}(\mathbb{S}^1)(\mathcal{V}_{\text{global}}) \propto \alpha_{\text{global}} \asymp \kappa^{-1/2}. \quad (21)$$

For directions $v \in \mathcal{V}_{\text{global}}$, their contribution to the contraction rate (20)

$$\left(e_1 \cdot \frac{\mathcal{C}^{-1/2}v}{|\mathcal{C}^{-1/2}v|} \right)^2 \geq \cos^2 \phi(\alpha_{\text{global}})$$

is bounded below resulting in the ballistic rate. It is precisely these global moves that enable Hit-and-Run to contract ballistically. On the other hand, directions in $\mathcal{V}_{\text{local}}$ contribute only a diffusive rate. In particular, for $\pi/2 - \alpha_{\text{global}} \leq 1$, the contribution from $\mathcal{V}_{\text{local}}$ is proportional to

$$\int_{\alpha_{\text{global}}}^{\pi/2} \frac{d\alpha}{\kappa \tan^2 \alpha + 1} \leq \int_{\alpha_{\text{global}}}^{\pi/2} \frac{d\alpha}{\frac{\kappa}{4(\pi/2-\alpha)^2} + 1} \leq \frac{\frac{\pi}{2} - \alpha_{\text{global}}}{\frac{\kappa}{4(\pi/2-\alpha_{\text{global}})^2} + 1} \asymp \kappa^{-1} \left(\frac{\pi}{2} - \alpha_{\text{global}} \right)^3 \leq \kappa^{-1}. \quad (22)$$

Thus, restricting to directions in $\mathcal{V}_{\text{local}}$ yields only a diffusive rate.

Three dimensions: One low mode Consider $\mathcal{C} = \text{diag}(\kappa, 1, 1)$, i.e., a three-dimensional Gaussian with two high and one low mode with respect to \mathcal{C}^{-1} . Due to rotational symmetry around e_1 , Figure 5 carries over to the distribution of directions on \mathbb{S}^2 so that \mathcal{Z} remains $\{\pm e_1\}$ and

$$\rho = \frac{1}{2} \mathbb{E}_{v \sim \sigma_2} \left(e_1 \cdot \frac{\mathcal{C}^{-1/2}v}{|\mathcal{C}^{-1/2}v|} \right)^2.$$

However, since the surface area of a spherical cap on \mathbb{S}^2 scales quadratically in its radius, in contrast to the linear scaling encountered in (21), it holds

$$\text{Unif}(\mathbb{S}^2)(\mathcal{V}_{\text{global}}) \propto \alpha_{\text{global}}^2 \asymp \kappa^{-1}$$

suggesting global moves to appear too seldom for ballistic contraction. Indeed, the rate computes to

$$\rho = \frac{1}{2} \frac{2}{4\pi} \int_0^{\pi/2} \cos^2 \phi(\alpha) 2\pi \sin \alpha d\alpha = \frac{1}{2} \int_0^{\pi/2} \frac{\sin \alpha}{\kappa \tan^2 \alpha + 1} d\alpha \asymp \kappa^{-1} \log \kappa$$

uncovering a superdiffusive scaling.

Three dimensions: One high mode Replacing one high mode by another low mode in the previous case, i.e., considering $\mathcal{C} = \text{diag}(\kappa, \kappa, 1)$, yields a three-dimensional Gaussian with rotational symmetry around e_3 . Then, the set of directions achieving the infimum in (11) becomes $\mathcal{Z} = \{\zeta \in \mathbb{S}^2 : \zeta \cdot e_3 = 0\}$, which corresponds to the equator of the sphere. This expands $\mathcal{V}_{\text{global}}$ to a neighborhood of the equator, for which, similarly to (21),

$$\text{Unif}(\mathbb{S}^2)(\mathcal{V}_{\text{global}}) \propto \alpha_{\text{global}} \asymp \kappa^{-1/2}.$$

As a result, Hit-and-Run again achieves ballistic contraction due to global moves with rate

$$\rho \asymp \kappa^{-1/2}.$$

Four dimensions: One low mode We found that in three dimensions with only one low mode, the contraction rate becomes superdiffusive. To understand how this behavior changes with increasing dimension, we consider the four-dimensional Gaussian with one low mode, i.e., $\mathcal{C} = \text{diag}(\kappa, 1, 1, 1)$. In this case, the infimum in the rate is again realized in $\zeta = e_1$. Using spherical coordinates,

$$\rho = \frac{1}{2} \mathbb{E}_{v \sim \sigma_3} \frac{\kappa^{-1} v_1^2}{|v|^2 - (1 - \kappa^{-1}) v_1^2} = \frac{1}{\pi} \int_0^\pi \frac{\kappa^{-1} \cos^2 s \sin^2 s}{1 - (1 - \kappa^{-1}) \cos^2 s} ds = \frac{\kappa^{-1}}{2(1 + \kappa^{-1/2})^2} \asymp \kappa^{-1}.$$

Thus, the contraction rate is diffusive. This suggests that Hit-and-Run contracts diffusively in high-dimensional Gaussians when the number of low modes is small.

High dimension After understanding that Hit-and-Run contracts diffusively in low dimensions with too few low modes, we examine high-dimensional, two-scale Gaussians with d_1 low and d_2 high modes, i.e.,

$$\mathcal{C} = \begin{pmatrix} \kappa I_{d_1} & 0 \\ 0 & I_{d_2} \end{pmatrix}.$$

The contraction rate in (11) can be expressed as

$$\rho = \frac{1}{2} \inf_{|\zeta|=1} \mathbb{E}_{v \sim \gamma_{d_1+d_2}} \left(\zeta \cdot \frac{\mathcal{C}^{-1/2} v}{|\mathcal{C}^{-1/2} v|} \right)^2 = \frac{1}{2} \inf_{|\zeta^1|^2 + |\zeta^2|^2 = 1} \mathbb{E}_{v^1 \sim \gamma_{d_1}} \mathbb{E}_{v^2 \sim \gamma_{d_2}} \frac{(\kappa^{-1/2} \zeta^1 \cdot v^1 + \zeta^2 \cdot v^2)^2}{\kappa^{-1} |v^1|^2 + |v^2|^2}$$

where we replaced the expectation over $\sigma_{d_1+d_2-1}$ with an expectation over the $(d_1 + d_2)$ -dimensional canonical Gaussian measure $\gamma_{d_1+d_2}$ normalized to the unit sphere. When d_1 and d_2 are large, $|v^1|^2 \approx d_1$ and $|v^2|^2 \approx d_2$ with high probability for $v^1 \sim \gamma_{d_1}$ and $v^2 \sim \gamma_{d_2}$. Substituting these approximations into the rate, we have

$$\begin{aligned} \rho &\approx \frac{1}{2} \inf_{|\zeta^1|^2 + |\zeta^2|^2 = 1} \frac{\kappa^{-1} \mathbb{E}_{v^1 \sim \gamma_{d_1}} (\zeta^1 \cdot v^1)^2 + \mathbb{E}_{v^2 \sim \gamma_{d_2}} (\zeta^2 \cdot v^2)^2}{\kappa^{-1} d_1 + d_2} = \frac{1}{2} \inf_{|\zeta^1|^2 + |\zeta^2|^2 = 1} \frac{\kappa^{-1} |\zeta^1|^2 + |\zeta^2|^2}{\kappa^{-1} d_1 + d_2} \\ &= \frac{1}{2} \frac{\kappa^{-1}}{\kappa^{-1} d_1 + d_2} = \frac{1}{2} (d_1 + \kappa d_2)^{-1}. \end{aligned}$$

We therefore expect Hit-and-Run to contract ballistically only in the regime $d_2 = \mathcal{O}(\kappa^{-1/2} d_1)$, i.e., if the relative number of high modes d_2 is sufficiently small relative to the number of low modes d_1 .

3.4 Mixing of Hit-and-Run

After proving and discussing the sharp Wasserstein contraction with rate ρ of Hit-and-Run, we now combine this result with a one-step overlap bound to obtain a mixing time upper bound. The following theorem states that Hit-and-Run mixes at a rate proportional to its Wasserstein contraction rate, i.e., the mixing time is of order ρ^{-1} up to logarithmic factors. Let $\mathcal{P}(\mathbb{R}^d)$ denote the collection of all probability measures on \mathbb{R}^d .

Theorem 2. Let $\varepsilon > 0$, $\nu \in \mathcal{P}(\mathbb{R}^d)$ and ρ as defined in (11). Then, there exist absolute constants $C, C' > 0$ such that the mixing time of Hit-and-Run with respect to the Gaussian measure $\gamma^{\mathcal{C}}$ starting from ν to accuracy ε satisfies

$$\begin{aligned} \tau_{\text{mix}}(\varepsilon, \nu) &= \inf\{n \in \mathbb{N} : \text{TV}(\nu \pi_{\text{H\&R}}^n, \gamma^{\mathcal{C}}) \leq \varepsilon\} \\ &\leq C \rho^{-1} \log\left(C' \max(\kappa, M, m^{-1}) d \varepsilon^{-1} \mathcal{W}_{\mathcal{C}^{-1/2}}^2(\gamma^{\mathcal{C}}, \nu)\right) \end{aligned} \quad (23)$$

where κ, M, m denote condition number, largest and smallest eigenvalue of \mathcal{C}^{-1} .

In Section 3.5, we prove a one-step overlap bound that essentially relates the total variation distance after a transition of Hit-and-Run to the Wasserstein distance prior to the transition. Using this result, the total variation distance to stationarity after n transitions can be controlled in terms of the Wasserstein distance to stationarity after $n - 1$ transitions, which decays exponentially with rate proportional to ρ . This leads to the mixing time upper bound stated in Theorem 2, whose detailed proof is given at the end of Section 3.5. Similar approaches to bounding mixing times have been employed in previous works [31, 26, 13, 27, 5, 6].

3.5 One-Step Overlap of Hit-and-Run

Here, we develop a total variation upper bound, which shows the transitions of Hit-and-Run in the target distribution $\gamma^{\mathcal{C}}$ to have a regularizing effect. Even for the Gaussian target measure, the transitions of Hit-and-Run are not Gaussian, see Figure 6. As a result, existing formulas cannot be directly applied, and new arguments must be developed.

Lemma 4. For any $\varepsilon \in (0, 1)$ and $x, \tilde{x} \in \mathbb{R}^d$,

$$\text{TV}(\pi_{\text{H\&R}}(x, \cdot), \pi_{\text{H\&R}}(\tilde{x}, \cdot)) \leq \sqrt{2} \left(C_1(x)^{1/2} |x - \tilde{x}|_{\mathcal{C}^{-1/2}} + C_2(x)^{1/2} |x - \tilde{x}|_{\mathcal{C}^{-1/2}}^{1/2} + C_3(x) \varepsilon^{1/2} \right)$$

where we have introduced

$$\begin{aligned} C_1(x) &= \varepsilon^{-1} m^{-1/2} |x|_{\mathcal{C}^{-1/2}} + 2\varepsilon M^{1/2} + 1, \\ C_2(x) &= 2\varepsilon^{-1} m^{-1/2} |x|_{\mathcal{C}^{-1/2}}^2 + 2|x|_{\mathcal{C}^{-1/2}} + (\varepsilon^{-1} m^{-1/2} + 2\varepsilon \kappa^{1/2})(d - 1) \\ &\quad + 2\varepsilon^{-1} m^{-1/2} + (M^{1/2} + m^{-1/2} + 2)\kappa^{1/2}, \\ C_3(x) &= \sqrt{3} M^{1/4} |x|_{\mathcal{C}^{-1/2}} + \sqrt{2} (1 + \log \varepsilon^{-1})^{1/2} M^{1/4} \sqrt{d - 1} + \sqrt{2} M^{1/4} (M^{1/2} + m^{-1/2} + 2)^{1/2}. \end{aligned}$$

The proof uses Pinsker's inequality, which states that for any probability measures $\nu, \eta \in \mathcal{P}(\mathbb{R}^d)$,

$$\text{TV}(\eta, \nu) \leq \sqrt{2} \mathcal{H}(\eta | \nu)^{1/2}, \quad (24)$$

where the relative entropy of η with respect to ν , $H(\eta | \nu) \in [0, \infty]$, is defined as

$$\mathcal{H}(\eta | \nu) = \begin{cases} \int \log \frac{d\eta}{d\nu} d\eta & \text{if } \eta \ll \nu, \\ \infty & \text{otherwise.} \end{cases} \quad (25)$$

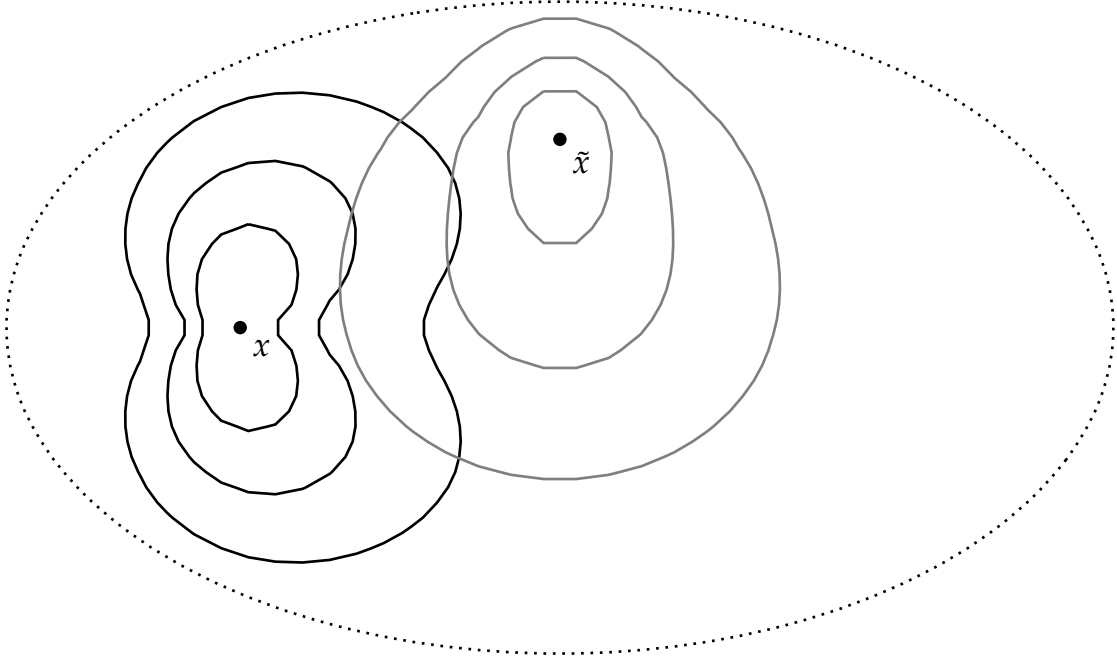


Figure 6: This figure shows contour lines of the transition density of the Hit-and-Run kernel in (26) starting from two different points: $x = (-2, 0)$ (black) and $\tilde{x} = (0, 1)$ (gray). The covariance matrix is $C = \text{diag}(4, 1)$. A contour line of the target density (dotted) is included for comparison.

To compute the relative entropy between two Hit-and-Run transition kernels starting at different initial points, we use the transition kernel's representation (4) in Cartesian coordinates and insert (6), which yields

$$\begin{aligned} \pi_{\text{H\&R}}(x, dy) &= 1_{\{y \neq x\}} \frac{2}{a_{d-1}} \frac{1}{|y-x|^{d-1}} \gamma_{x, \frac{y-x}{|y-x|}}^C(|y-x|) dy \\ &= 1_{\{y \neq x\}} \frac{2}{a_{d-1}} \frac{|\mathcal{C}^{-1/2}(y-x)|}{\sqrt{2\pi} |y-x|^d} \exp\left(-\frac{|\mathcal{C}^{-1/2}y|^2}{2} + \frac{|\mathcal{C}^{-1/2}x|^2}{2} - \frac{(x \cdot \mathcal{C}^{-1}(y-x))^2}{2|\mathcal{C}^{-1/2}(y-x)|^2}\right) dy. \end{aligned} \quad (26)$$

Proof. Using (26), we decompose the relative entropy of $\pi_{\text{H\&R}}(x, \cdot)$ with respect to $\pi_{\text{H\&R}}(\tilde{x}, \cdot)$ as

$$\begin{aligned} \mathcal{H}(\pi_{\text{H\&R}}(x, \cdot) | \pi_{\text{H\&R}}(\tilde{x}, \cdot)) &= \text{I} + \text{II} + \text{III} + \text{IV} \quad \text{where} \quad (27) \\ \text{I} &= \frac{|\mathcal{C}^{-1/2}x|^2}{2} - \frac{|\mathcal{C}^{-1/2}\tilde{x}|^2}{2}, \\ \text{II} &= \int_{\mathbb{R}^d} \left(\frac{(\tilde{x} \cdot \mathcal{C}^{-1}(y-\tilde{x}))^2}{2|\mathcal{C}^{-1/2}(y-\tilde{x})|^2} - \frac{(x \cdot \mathcal{C}^{-1}(y-x))^2}{2|\mathcal{C}^{-1/2}(y-x)|^2} \right) \pi_{\text{H\&R}}(x, dy), \\ \text{III} &= (d-1) \int_{\mathbb{R}^d} \log \frac{|y-\tilde{x}|}{|y-x|} \pi_{\text{H\&R}}(x, dy), \\ \text{IV} &= \int_{\mathbb{R}^d} \left(\log \frac{|\mathcal{C}^{-1/2}(y-x)|}{|y-x|} + \log \frac{|y-\tilde{x}|}{|\mathcal{C}^{-1/2}(y-\tilde{x})|} \right) \pi_{\text{H\&R}}(x, dy). \end{aligned}$$

The first term, I, can be estimated directly using the reverse triangle inequality:

$$\begin{aligned} \text{I} &= \frac{1}{2} (|\mathcal{C}^{-1/2}x| + |\mathcal{C}^{-1/2}\tilde{x}|) (|\mathcal{C}^{-1/2}x| - |\mathcal{C}^{-1/2}\tilde{x}|) , \\ &\leq \frac{1}{2} (2|\mathcal{C}^{-1/2}x| + |\mathcal{C}^{-1/2}(x - \tilde{x})|) |\mathcal{C}^{-1/2}(x - \tilde{x})| . \end{aligned} \quad (28)$$

To bound the remaining terms in (27), we split each integral into two parts using an indicator function for the set $A_{x,\epsilon} = \{y \in \mathbb{R}^d : |y - x| > \epsilon\}$ and its complement $A_{x,\epsilon}^c = \mathbb{R}^d \setminus A_{x,\epsilon}$, where $\epsilon > 0$. Additionally, from (3) and (6), we can bound the probability to transition to $A_{x,\epsilon}^c$ as follows:

$$\begin{aligned} \pi_{\text{H\&R}}(x, A_{x,\epsilon}^c) &= \int_{\mathbb{S}^{d-1}} \int_{\mathbb{R}} \mathbf{1}_{A_{x,\epsilon}^c}(x + hv) \gamma_{x,v}^{\mathcal{C}}(dh) \sigma_{d-1}(dv) = \int_{\mathbb{S}^{d-1}} \int_{-\epsilon}^{\epsilon} \gamma_{x,v}^{\mathcal{C}}(dh) \sigma_{d-1}(dv) \\ &\leq \int_{\mathbb{S}^{d-1}} \int_{-\epsilon}^{\epsilon} dh |\mathcal{C}^{-1/2}v| \sigma_{d-1}(dv) \leq 2\epsilon \sup_{|v|=1} |\mathcal{C}^{-1/2}v| \leq 2\epsilon M^{1/2} , \end{aligned} \quad (29)$$

where $M^{1/2}$ is the largest eigenvalue of $\mathcal{C}^{-1/2}$. Similarly, we can bound

$$\begin{aligned} \int_{A_{x,\epsilon}^c} \log |y - x|^{-1} \pi_{\text{H\&R}}(x, dy) &= \int_{\mathbb{S}^{d-1}} \int_{-\epsilon}^{\epsilon} \log |h|^{-1} \gamma_{x,v}^{\mathcal{C}}(dh) \sigma_{d-1}(dv) \\ &\leq \int_{\mathbb{S}^{d-1}} \int_{-\epsilon}^{\epsilon} \log |h|^{-1} dh |\mathcal{C}^{-1/2}v| \sigma_{d-1}(dv) \leq 2\epsilon(1 - \log \epsilon) M^{1/2} . \end{aligned} \quad (30)$$

The bounds (29) and (30) will be useful to estimate the remaining terms in the region $A_{x,\epsilon}^c$.

Specifically, we decompose the second term, II, as follows:

$$\begin{aligned} \text{II} &= \text{II}_a + \text{II}_b \quad \text{where} \\ \text{II}_a &= \frac{1}{2} \int_{A_{x,\epsilon}} \left(\frac{(\tilde{x} \cdot \mathcal{C}^{-1}(y - \tilde{x}))^2}{|\mathcal{C}^{-1/2}(y - \tilde{x})|^2} - \frac{(x \cdot \mathcal{C}^{-1}(y - x))^2}{|\mathcal{C}^{-1/2}(y - x)|^2} \right) \pi_{\text{H\&R}}(x, dy) , \\ \text{II}_b &= \frac{1}{2} \int_{A_{x,\epsilon}^c} \left(\frac{(\tilde{x} \cdot \mathcal{C}^{-1}(y - \tilde{x}))^2}{|\mathcal{C}^{-1/2}(y - \tilde{x})|^2} - \frac{(x \cdot \mathcal{C}^{-1}(y - x))^2}{|\mathcal{C}^{-1/2}(y - x)|^2} \right) \pi_{\text{H\&R}}(x, dy) . \end{aligned} \quad (31)$$

The term II_a involves a difference of two squares. The first factor in this difference can be bounded by using the Cauchy-Schwarz and triangle inequality:

$$\begin{aligned} \text{II}_a &= \frac{1}{2} \int_{A_{x,\epsilon}} \left(\frac{\tilde{x} \cdot \mathcal{C}^{-1}(y - \tilde{x})}{|\mathcal{C}^{-1/2}(y - \tilde{x})|} + \frac{x \cdot \mathcal{C}^{-1}(y - x)}{|\mathcal{C}^{-1/2}(y - x)|} \right) \\ &\quad \times \left(\frac{\tilde{x} \cdot \mathcal{C}^{-1}(y - \tilde{x})}{|\mathcal{C}^{-1/2}(y - \tilde{x})|} - \frac{x \cdot \mathcal{C}^{-1}(y - x)}{|\mathcal{C}^{-1/2}(y - x)|} \right) \pi_{\text{H\&R}}(x, dy) , \\ &\leq \frac{1}{2} (2|\mathcal{C}^{-1/2}x| + |\mathcal{C}^{-1/2}(x - \tilde{x})|) \\ &\quad \times \int_{A_{x,\epsilon}} \left| \frac{\tilde{x} \cdot \mathcal{C}^{-1}(y - \tilde{x})}{|\mathcal{C}^{-1/2}(y - \tilde{x})|} - \frac{x \cdot \mathcal{C}^{-1}(y - x)}{|\mathcal{C}^{-1/2}(y - x)|} \right| \pi_{\text{H\&R}}(x, dy) . \end{aligned} \quad (32)$$

The integrand in (32) can also be bounded by using the Cauchy-Schwarz and triangle inequalities

$$\begin{aligned}
& \left| \frac{\tilde{x} \cdot \mathcal{C}^{-1}(\mathbf{y} - \tilde{x})}{|\mathcal{C}^{-1/2}(\mathbf{y} - \tilde{x})|} - \frac{x \cdot \mathcal{C}^{-1}(\mathbf{y} - x)}{|\mathcal{C}^{-1/2}(\mathbf{y} - x)|} \right| \leq |\mathcal{C}^{-1/2}(x - \tilde{x})| + \left| \frac{x \cdot \mathcal{C}^{-1}(\mathbf{y} - \tilde{x})}{|\mathcal{C}^{-1/2}(\mathbf{y} - \tilde{x})|} - \frac{x \cdot \mathcal{C}^{-1}(\mathbf{y} - x)}{|\mathcal{C}^{-1/2}(\mathbf{y} - x)|} \right| \\
& \leq |\mathcal{C}^{-1/2}(x - \tilde{x})| + |\mathcal{C}^{-1/2}x| \left| \frac{\mathcal{C}^{-1/2}(\mathbf{y} - \tilde{x})}{|\mathcal{C}^{-1/2}(\mathbf{y} - \tilde{x})|} - \frac{\mathcal{C}^{-1/2}(\mathbf{y} - x)}{|\mathcal{C}^{-1/2}(\mathbf{y} - x)|} + \frac{\mathcal{C}^{-1/2}(x - \tilde{x})}{|\mathcal{C}^{-1/2}(\mathbf{y} - x)|} \right| \\
& \leq |\mathcal{C}^{-1/2}(x - \tilde{x})| + |\mathcal{C}^{-1/2}x| \left(\left| \frac{\mathcal{C}^{-1/2}(\mathbf{y} - \tilde{x})}{|\mathcal{C}^{-1/2}(\mathbf{y} - \tilde{x})|} - \frac{\mathcal{C}^{-1/2}(\mathbf{y} - x)}{|\mathcal{C}^{-1/2}(\mathbf{y} - x)|} \right| + \left| \frac{\mathcal{C}^{-1/2}(x - \tilde{x})}{|\mathcal{C}^{-1/2}(\mathbf{y} - x)|} \right| \right) \\
& = |\mathcal{C}^{-1/2}(x - \tilde{x})| + \frac{|\mathcal{C}^{-1/2}x|}{|\mathcal{C}^{-1/2}(\mathbf{y} - x)|} \left(\left| |\mathcal{C}^{-1/2}(\mathbf{y} - x)| - |\mathcal{C}^{-1/2}(\mathbf{y} - \tilde{x})| \right| + |\mathcal{C}^{-1/2}(x - \tilde{x})| \right) \\
& \leq \left(1 + \frac{2}{\epsilon m^{1/2}} |\mathcal{C}^{-1/2}x| \right) |\mathcal{C}^{-1/2}(x - \tilde{x})| \tag{33}
\end{aligned}$$

where in the last step we used that $|\mathcal{C}^{-1/2}(\mathbf{y} - x)| \geq \epsilon m^{1/2}$ in $A_{x,\epsilon}$. Inserting the bound (33) back into (32) gives

$$\begin{aligned}
\Pi_a & \leq \frac{1}{2} \left(2|\mathcal{C}^{-1/2}x| + |\mathcal{C}^{-1/2}(x - \tilde{x})| \right) \left(1 + \frac{2}{\epsilon m^{1/2}} |\mathcal{C}^{-1/2}x| \right) |\mathcal{C}^{-1/2}(x - \tilde{x})| \\
& \leq \left(|\mathcal{C}^{-1/2}x| + \frac{2}{\epsilon m^{1/2}} |\mathcal{C}^{-1/2}x|^2 \right) |\mathcal{C}^{-1/2}(x - \tilde{x})| + \frac{1}{2} \left(1 + \frac{2}{\epsilon m^{1/2}} |\mathcal{C}^{-1/2}x| \right) |\mathcal{C}^{-1/2}(x - \tilde{x})|^2. \tag{34}
\end{aligned}$$

On the other hand, by again using the Cauchy-Schwarz, triangle inequalities and (29)

$$\begin{aligned}
\Pi_b & \leq \frac{1}{2} \int_{A_{x,\epsilon}^c} \left(\left| \frac{\tilde{x} \cdot \mathcal{C}^{-1}(\mathbf{y} - \tilde{x})}{|\mathcal{C}^{-1/2}(\mathbf{y} - \tilde{x})|} \right|^2 + \left| \frac{x \cdot \mathcal{C}^{-1}(\mathbf{y} - x)}{|\mathcal{C}^{-1/2}(\mathbf{y} - \tilde{x})|} \right|^2 \right) \pi_{\text{H\&R}}(x, d\mathbf{y}) \\
& \leq \frac{1}{2} (|\mathcal{C}^{-1/2}\tilde{x}|^2 + |\mathcal{C}^{-1/2}x|^2) \pi_{\text{H\&R}}(x, A_{x,\epsilon}^c) \leq 2\epsilon M^{1/2} |\mathcal{C}^{-1/2}(x - \tilde{x})|^2 + 3\epsilon M^{1/2} |\mathcal{C}^{-1/2}x|^2. \tag{35}
\end{aligned}$$

Inserting (34) and (35) into (31) yields

$$\begin{aligned}
\Pi & \leq \left(|\mathcal{C}^{-1/2}x| + \frac{2}{\epsilon m^{1/2}} |\mathcal{C}^{-1/2}x|^2 \right) |\mathcal{C}^{-1/2}(x - \tilde{x})| \\
& \quad + \left(\frac{1}{2} + 2\epsilon M^{1/2} + \frac{1}{\epsilon m^{1/2}} |\mathcal{C}^{-1/2}x| \right) |\mathcal{C}^{-1/2}(x - \tilde{x})|^2 + 3\epsilon M^{1/2} |\mathcal{C}^{-1/2}x|^2. \tag{36}
\end{aligned}$$

Likewise, we can decompose the third term, III , as:

$$\begin{aligned}
\text{III} & = \text{III}_a + \text{III}_b \quad \text{where} \tag{37} \\
\text{III}_a & = (d-1) \int_{A_{x,\epsilon}} \log \frac{|\mathbf{y} - \tilde{x}|}{|\mathbf{y} - x|} \pi_{\text{H\&R}}(x, d\mathbf{y}), \\
\text{III}_b & = (d-1) \int_{A_{x,\epsilon}^c} \log \frac{|\mathbf{y} - \tilde{x}|}{|\mathbf{y} - x|} \pi_{\text{H\&R}}(x, d\mathbf{y}).
\end{aligned}$$

Applying the elementary inequality

$$\log(x) \leq x - 1 \quad \text{for } x > 0 \tag{38}$$

in III_a gives

$$\begin{aligned}\text{III}_a &\leq (d-1) \int_{A_{x,\epsilon}} \left(\frac{|y-\tilde{x}|}{|y-x|} - 1 \right) \pi_{\text{H\&R}}(x, dy) \leq (d-1) \int_{A_{x,\epsilon}} \frac{||y-\tilde{x}|-|y-x||}{|y-x|} \pi_{\text{H\&R}}(x, dy) \\ &\leq (d-1) \frac{|x-\tilde{x}|}{\epsilon} \leq \frac{(d-1)m^{-1/2}}{\epsilon} |\mathcal{C}^{-1/2}(x-\tilde{x})|, \end{aligned} \quad (39)$$

where we used the triangle inequality, $|y-x| \geq \epsilon$ for $y \in A_{x,\epsilon}$, and $|x-\tilde{x}| \leq m^{-1/2}|\mathcal{C}^{-1/2}(x-\tilde{x})|$.

On the other hand, for $y \in A_{x,\epsilon}^c$, we have $|y-x| \leq \epsilon$. In this case, we further decompose $\text{III}_b = \text{III}_{b,1} + \text{III}_{b,2}$ where

$$\begin{aligned}\text{III}_{b,1} &= (d-1) \int_{A_{x,\epsilon}^c} \log |y-\tilde{x}| \pi_{\text{H\&R}}(x, dy), \\ \text{III}_{b,2} &= (d-1) \int_{A_{x,\epsilon}^c} \log |y-x|^{-1} \pi_{\text{H\&R}}(x, dy).\end{aligned}$$

For the first term, we use $|y-x| \leq \epsilon \leq 1$, as follows:

$$\begin{aligned}\text{III}_{b,1} &\leq (d-1) \int_{A_{x,\epsilon}^c} \log |y-\tilde{x}| \pi_{\text{H\&R}}(x, dy) \leq (d-1) \int_{A_{x,\epsilon}^c} \log(|y-x| + |x-\tilde{x}|) \pi_{\text{H\&R}}(x, dy) \\ &\leq (d-1) \log(1 + |x-\tilde{x}|) \pi_{\text{H\&R}}(x, A_{x,\epsilon}^c) \leq 2\epsilon M^{1/2} (d-1) |x-\tilde{x}| \\ &\leq 2\epsilon \kappa^{1/2} (d-1) |\mathcal{C}^{-1/2}(x-\tilde{x})|, \end{aligned} \quad (40)$$

where we used (38), (29), and $|x-\tilde{x}| \leq m^{-1/2}|\mathcal{C}^{-1/2}(x-\tilde{x})|$. For the second term, by (30)

$$\text{III}_{b,2} \leq (d-1) \int_{A_{x,\epsilon}^c} \log |y-x|^{-1} \pi_{\text{H\&R}}(x, dy) \leq 2\epsilon(1 - \log \epsilon) M^{1/2} (d-1). \quad (41)$$

Inserting (39), (40), and (41) into (37) yields

$$\text{III} \leq (d-1) \left((\epsilon^{-1} m^{-1/2} + 2\epsilon \kappa^{1/2}) |\mathcal{C}^{-1/2}(x-\tilde{x})| + 2\epsilon(1 - \log \epsilon) M^{1/2} \right). \quad (42)$$

Similarly, we can decompose the fourth term, IV , as

$$\begin{aligned}\text{IV} &= \text{IV}_a + \text{IV}_b \quad \text{where} \quad (43) \\ \text{IV}_a &= \int_{A_{x,\epsilon}} \left(\log \frac{|\mathcal{C}^{-1/2}(y-x)|}{|y-x|} + \log \frac{|y-\tilde{x}|}{|\mathcal{C}^{-1/2}(y-\tilde{x})|} \right) \pi_{\text{H\&R}}(x, dy), \\ \text{IV}_b &= \int_{A_{x,\epsilon}^c} \left(\log \frac{|\mathcal{C}^{-1/2}(y-x)|}{|y-x|} + \log \frac{|y-\tilde{x}|}{|\mathcal{C}^{-1/2}(y-\tilde{x})|} \right) \pi_{\text{H\&R}}(x, dy).\end{aligned}$$

For $y \in A_{x,\epsilon}$, we have $|y-x| \geq \epsilon$. In this case, we further decompose $\text{IV}_a = \text{IV}_{a,1} + \text{IV}_{a,2}$ as follows:

$$\begin{aligned}\text{IV}_{a,1} &= \int_{A_{x,\epsilon} \cap A_{\tilde{x},\epsilon}} \left(\log \frac{|\mathcal{C}^{-1/2}(y-x)|}{|\mathcal{C}^{-1/2}(y-\tilde{x})|} + \log \frac{|y-\tilde{x}|}{|y-x|} \right) \pi_{\text{H\&R}}(x, dy), \\ \text{IV}_{a,2} &= \int_{A_{x,\epsilon} \cap A_{\tilde{x},\epsilon}^c} \left(\log \frac{|\mathcal{C}^{-1/2}(y-x)|}{|y-x|} + \log \frac{|y-\tilde{x}|}{|\mathcal{C}^{-1/2}(y-\tilde{x})|} \right) \pi_{\text{H\&R}}(x, dy).\end{aligned}$$

By applying (38) and the triangle inequality, the first term can be bounded by

$$\begin{aligned}
\mathbb{IV}_{a,1} &\leq \int_{A_{x,\epsilon} \cap A_{\tilde{x},\epsilon}} \left(\frac{|\mathcal{C}^{-1/2}(y-x)| - |\mathcal{C}^{-1/2}(y-\tilde{x})|}{|\mathcal{C}^{-1/2}(y-\tilde{x})|} + \frac{|y-\tilde{x}| - |y-x|}{|y-x|} \right) \pi_{\text{H\&R}}(x, dy) \\
&\leq \int_{A_{x,\epsilon} \cap A_{\tilde{x},\epsilon}} \left(\frac{|\mathcal{C}^{-1/2}(x-\tilde{x})|}{|\mathcal{C}^{-1/2}(y-\tilde{x})|} + \frac{|x-\tilde{x}|}{|y-x|} \right) \pi_{\text{H\&R}}(x, dy) \\
&\leq \left(\frac{|\mathcal{C}^{-1/2}(x-\tilde{x})|}{\epsilon m^{1/2}} + \frac{|x-\tilde{x}|}{\epsilon} \right) \pi_{\text{H\&R}}(x, A_{x,\epsilon} \cap A_{\tilde{x},\epsilon}) \leq \frac{2}{\epsilon m^{1/2}} |\mathcal{C}^{-1/2}(x-\tilde{x})|. \quad (44)
\end{aligned}$$

For the second term, by again applying (38), and subsequently using that $\epsilon < |y-x| \leq \epsilon + |x-\tilde{x}|$ for $y \in A_{x,\epsilon} \cap A_{\tilde{x},\epsilon}^c$ in an estimate resembling (29),

$$\begin{aligned}
\mathbb{IV}_{a,2} &\leq \int_{A_{x,\epsilon} \cap A_{\tilde{x},\epsilon}^c} \left(\frac{|\mathcal{C}^{-1/2}(y-x)|}{|y-x|} + \frac{|y-\tilde{x}|}{|\mathcal{C}^{-1/2}(y-\tilde{x})|} - 2 \right) \pi_{\text{H\&R}}(x, dy) \\
&\leq |M^{1/2} + m^{-1/2} - 2| \pi_{\text{H\&R}}(x, A_{x,\epsilon} \cap A_{\tilde{x},\epsilon}^c) \\
&\leq (M^{1/2} + m^{-1/2} + 2) \int_{\mathbb{S}^{d-1}} \int_{\mathbb{R}} 1_{A_{x,\epsilon} \cap A_{\tilde{x},\epsilon}^c}(x+hv) \gamma_{x,v}^{\mathcal{C}}(dh) \sigma_{d-1}(dv) \\
&\leq (M^{1/2} + m^{-1/2} + 2) \int_{\mathbb{S}^{d-1}} \int_{\epsilon}^{\epsilon+|x-\tilde{x}|} dh |\mathcal{C}^{-1/2}v| \sigma_{d-1}(dv) \\
&\leq (M^{1/2} + m^{-1/2} + 2) \kappa^{1/2} |\mathcal{C}^{-1/2}(x-\tilde{x})|. \quad (45)
\end{aligned}$$

The last two displays together give

$$\mathbb{IV}_a \leq \left(\frac{2}{\epsilon m^{1/2}} + (M^{1/2} + m^{-1/2} + 2) \kappa^{1/2} \right) |\mathcal{C}^{-1/2}(x-\tilde{x})|. \quad (46)$$

On the other hand, by applying (38) and (29),

$$\begin{aligned}
\mathbb{IV}_b &\leq \int_{A_{\tilde{x},\epsilon}^c} \left(\frac{|\mathcal{C}^{-1/2}(y-x)|}{|y-x|} + \frac{|y-\tilde{x}|}{|\mathcal{C}^{-1/2}(y-\tilde{x})|} - 2 \right) \pi_{\text{H\&R}}(x, dy) \\
&\leq |M^{1/2} + m^{-1/2} - 2| \pi_{\text{H\&R}}(x, A_{\tilde{x},\epsilon}^c) \leq 2\epsilon M^{1/2} (M^{1/2} + m^{-1/2} + 2). \quad (47)
\end{aligned}$$

Inserting (46) and (47) into (43) yields

$$\mathbb{IV} \leq \left(\frac{2}{\epsilon m^{1/2}} + (M^{1/2} + m^{-1/2} + 2) \kappa^{1/2} \right) |\mathcal{C}^{-1/2}(x-\tilde{x})| + 2\epsilon M^{1/2} (M^{1/2} + m^{-1/2} + 2). \quad (48)$$

Inserting (28), (36), (42) and (48) into (27) yields

$$\begin{aligned}
\mathcal{H}(\pi_{\text{H\&R}}(x, \cdot) | \pi_{\text{H\&R}}(\tilde{x}, \cdot)) &\leq \left[\epsilon^{-1} m^{-1/2} |\mathcal{C}^{-1/2}x| + 2\epsilon M^{1/2} + 1 \right] |\mathcal{C}^{-1/2}(x-\tilde{x})|^2 \\
&\quad + \left[2\epsilon^{-1} m^{-1/2} |\mathcal{C}^{-1/2}x|^2 + 2|\mathcal{C}^{-1/2}x| + (\epsilon^{-1} m^{-1/2} + 2\epsilon \kappa^{1/2})(d-1) \right. \\
&\quad \left. + 2\epsilon^{-1} m^{-1/2} + (M^{1/2} + m^{-1/2} + 2) \kappa^{1/2} \right] |\mathcal{C}^{-1/2}(x-\tilde{x})| \\
&\quad + \left[3M^{1/2} |\mathcal{C}^{-1/2}x|^2 + 2(1 + \log \epsilon^{-1}) M^{1/2} (d-1) + 2M^{1/2} (M^{1/2} + m^{-1/2} + 2) \right] \epsilon.
\end{aligned}$$

Finally, inserting the last display into Pinsker's inequality (24) and using subadditivity of the square root, we obtain

$$\begin{aligned} \text{TV}(\pi_{\text{H\&R}}(x, \cdot), \pi_{\text{H\&R}}(\tilde{x}, \cdot)) &\leq \sqrt{2} \mathcal{H}(\pi_{\text{H\&R}}(x, \cdot) | \pi_{\text{H\&R}}(\tilde{x}, \cdot))^{1/2} \\ &\leq \sqrt{2} \left(C_1(x)^{1/2} |C^{-1/2}(x - \tilde{x})| + C_2(x)^{1/2} |C^{-1/2}(x - \tilde{x})|^{1/2} + C_3(x) \epsilon^{1/2} \right) \end{aligned}$$

finishing the proof. \square

We now extend the overlap bound of Lemma 4 to arbitrary initial distributions.

Lemma 5. *For any $\epsilon \in (0, 1)$ and $\eta, \nu \in \mathcal{P}(\mathbb{R}^d)$,*

$$\text{TV}(\eta \pi_{\text{H\&R}}, \nu \pi_{\text{H\&R}}) \leq \sqrt{2} \left((\eta(C_1))^{1/2} \mathcal{W}_{C^{-1/2}}^2(\eta, \nu) + (\eta(C_2))^{1/2} \mathcal{W}_{C^{-1/2}}^2(\eta, \nu)^{1/2} + \eta(C_3) \epsilon^{1/2} \right).$$

Proof of Lemma 5. Let (X, \tilde{X}) be an arbitrary coupling of η and ν . By the coupling characterization of the TV distance and Lemma 4,

$$\begin{aligned} \text{TV}(\eta \pi_{\text{H\&R}}, \nu \pi_{\text{H\&R}}) &\leq \mathbb{E} \text{TV}(\pi_{\text{H\&R}}(X, \cdot), \pi_{\text{H\&R}}(\tilde{X}, \cdot)) \\ &\leq \sqrt{2} \mathbb{E} \left(C_1(X)^{1/2} |X - \tilde{X}|_{C^{-1/2}} + C_2(X)^{1/2} |X - \tilde{X}|_{C^{-1/2}}^{1/2} + C_3(X) \epsilon^{1/2} \right). \end{aligned}$$

By Cauchy-Schwarz and Jensen's inequality,

$$\begin{aligned} \text{TV}(\eta \pi_{\text{H\&R}}, \nu \pi_{\text{H\&R}}) &\leq \sqrt{2} \left((\eta(C_1))^{1/2} (\mathbb{E} |X - \tilde{X}|_{C^{-1/2}}^2)^{1/2} \right. \\ &\quad \left. + (\eta(C_2))^{1/2} (\mathbb{E} |X - \tilde{X}|_{C^{-1/2}}^2)^{1/4} + \eta(C_3) \epsilon^{1/2} \right). \end{aligned}$$

Take the infimum over all couplings of η and ν to finish the proof. \square

After proving the required overlap bounds, we are positioned to prove the mixing time upper bound for Hit-and-Run.

Proof of Theorem 2. Let $C, C' > 0$ be an absolute constants that may change from line to line.

Inserting $\gamma^C(|x|_{C^{-1/2}}^2) = d$ and $\gamma^C(|x|_{C^{-1/2}}) \leq d^{1/2}$ into the constants of Lemma 4 yields

$$\gamma^C(C_1) \leq C \max(\kappa, M, m^{-1})^{1/2} d^{1/2} \epsilon^{-1}, \quad (49)$$

$$\gamma^C(C_2) \leq C \max(\kappa, M, m^{-1}) d \epsilon^{-1}, \quad (50)$$

$$\gamma^C(C_3) \epsilon^{1/2} \leq C \max(\kappa, M, m^{-1})^{1/2} d^{1/2} (1 + \log \epsilon^{-1})^{1/2} \epsilon^{1/2}. \quad (51)$$

Combining Lemma 2 and Lemma 5, we see for any $\nu \in \mathcal{P}(\mathbb{R}^d)$ and any $n \in \mathbb{N}$

$$\begin{aligned} \text{TV}(\gamma^C, \nu \pi_{\text{H\&R}}^{n+1}) &= \text{TV}(\gamma^C \pi_{\text{H\&R}}^{n+1}, \nu \pi_{\text{H\&R}}^{n+1}) \\ &\leq \sqrt{2} \left((\gamma^C(C_1))^{1/2} \mathcal{W}_{C^{-1/2}}^2(\gamma^C, \nu) e^{-\rho n} + (\gamma^C(C_2))^{1/2} \mathcal{W}_{C^{-1/2}}^2(\gamma^C, \nu)^{1/2} e^{-\rho n/2} + \gamma^C(C_3) \epsilon^{1/2} \right). \end{aligned}$$

The right hand side is bounded above by $\varepsilon > 0$ if the following three bounds hold:

$$(\gamma^{\mathcal{C}}(C_1))^{1/2} \mathcal{W}_{\mathcal{C}^{-1/2}}^2(\gamma^{\mathcal{C}}, \nu) e^{-\rho n} \leq \frac{\varepsilon}{3\sqrt{2}}, \quad (52)$$

$$(\gamma^{\mathcal{C}}(C_2))^{1/2} \mathcal{W}_{\mathcal{C}^{-1/2}}^2(\gamma^{\mathcal{C}}, \nu)^{1/2} e^{-\rho n/2} \leq \frac{\varepsilon}{3\sqrt{2}}, \quad (53)$$

$$\gamma^{\mathcal{C}}(C_3) \varepsilon^{1/2} \leq \frac{\varepsilon}{3\sqrt{2}}. \quad (54)$$

Using $(1 + \log \varepsilon^{-1})\varepsilon \leq 2\varepsilon^{1/2}$ in (51), we see that (54) holds for

$$\varepsilon = C \max(\kappa, M, m^{-1})^{-2} d^{-2} \varepsilon^4 \quad \text{with a suitable absolute constant } C.$$

Inserting this choice into (49) and (50) yields

$$\max(\gamma^{\mathcal{C}}(C_1), \gamma^{\mathcal{C}}(C_2)) \leq C \max(\kappa, M, m^{-1})^3 d^3 \varepsilon^{-4}.$$

As conditions (52) and (53) are guaranteed for

$$n \geq C\rho^{-1} \log\left(C' \max(\gamma^{\mathcal{C}}(C_1), \gamma^{\mathcal{C}}(C_2)) \varepsilon^{-1} \mathcal{W}_{\mathcal{C}^{-1/2}}^2(\gamma^{\mathcal{C}}, \nu)\right)$$

with suitable absolute constants C, C' , the mixing time satisfies

$$\tau_{\text{mix}}(\varepsilon, \nu) \leq C\rho^{-1} \log\left(C' \max(\kappa, M, m^{-1}) d \varepsilon^{-1} \mathcal{W}_{\mathcal{C}^{-1/2}}^2(\gamma^{\mathcal{C}}, \nu)\right).$$

□

4 Coordinate-free randomized Kaczmarz algorithm

The Kaczmarz algorithm [20, 17, 18] is an iterative method for approximately solving overdetermined linear systems of the form

$$Ax = b \quad (55)$$

where $A \in \mathbb{R}^{d \times m}$ is a full rank matrix with $d \geq m$, and $b \in \mathbb{R}^d$. The algorithm leverages the geometric interpretation of the solution to (55) as the intersection of the hyperplanes

$$H_i = \{x \in \mathbb{R}^m : e_i \cdot (Ax - b) = 0\} \quad \text{for } 1 \leq i \leq d \quad (56)$$

where e_i is the i -th canonical basis vector of \mathbb{R}^d .

Starting from an initial state $x_0 \in \mathbb{R}^m$, the Kaczmarz method iteratively updates the solution. At each iteration, a basis vector e_i is selected, and the next state x_{k+1} is computed as the orthogonal projection of the current state x_k onto the corresponding hyperplane H_i . The classical Kaczmarz method selects the basis vectors deterministically in a cyclic order [20].

Strohmer and Vershynin [36] later introduced and analyzed a randomized variant of the Kaczmarz method, where the basis vectors are selected randomly, with probabilities proportional to $|A^T e_i|^2$. They provided a sharp bound on the mean-squared convergence to the solution of (55).

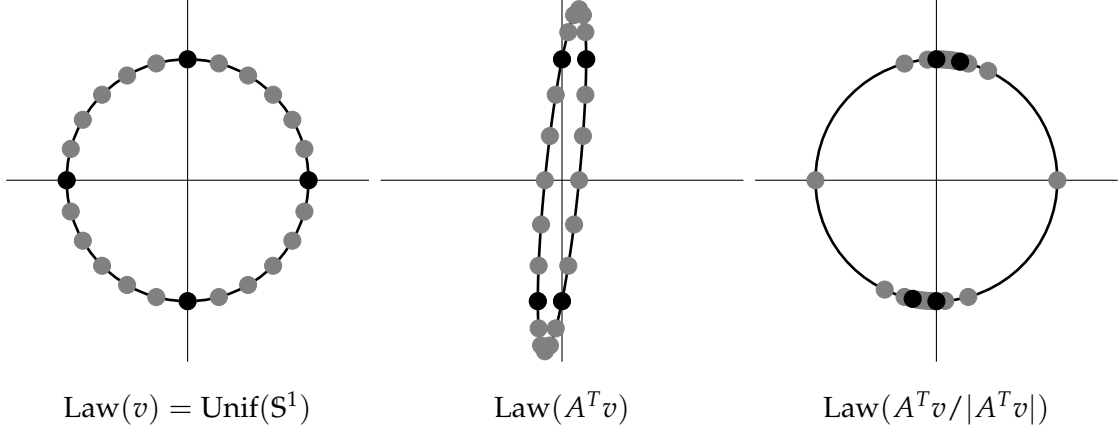


Figure 7: Distribution of the directions $A^T v / |A^T v|$, $v \sim \text{Unif}(\mathbb{S}^1)$, along which coordinate-free randomized Kaczmarz moves, for A as in (59). The gray beads illustrate the redistribution of probability mass, favoring directions nearly orthogonal to e_1 (resulting in local moves along e_1) while retaining enough mass in directions allowing global moves along e_1 . This enables the coordinate-free method to converge at the ballistic rate in (61). In contrast, the black beads represent the fixed directions to which randomized Kaczmarz is restricted, explaining its slower, diffusive rate in (60).

In each iteration, the direction of update in the randomized Kaczmarz method is restricted to $\text{span}(A^T e_i)$, i.e., normal to the selected hyperplane H_i . Analogously, the random-scan Gibbs sampler is restricted to move in $\text{span}(e_i)$, corresponding to a randomly selected basis vector. The possible improvement from diffusive to ballistic mixing in Hit-and-Run — achieved by allowing random-scan Gibbs to move in any coordinate-free, randomly sampled direction $v \in \mathbb{S}^{d-1}$ — motivates us to consider a similar coordinate-free extension for the randomized Kaczmarz algorithm.

We begin by generalizing (56) from coordinate-bound unit vectors to coordinate-free unit vectors. Specifically, the solution to (55) can be expressed as the intersection of the hyperplanes

$$H(v) = \{x \in \mathbb{R}^m : v \cdot (Ax - b) = 0\} \quad \text{for } v \in \mathbb{S}^{d-1}.$$

Let τ be a probability measure on \mathbb{S}^{d-1} . The iterations of the *generalized randomized Kaczmarz algorithm* are defined as follows: select $v \sim \tau$, then compute the updated state x_{k+1} by projecting the current state x_k orthogonally onto $H(v)$. Since

$$H(v) = \text{span}(A^T v)^\perp + \frac{v \cdot b}{|A^T v|} \frac{A^T v}{|A^T v|},$$

the update step can be written explicitly as

$$x_{k+1} = \Pi_{A^T v} x_k + \frac{v \cdot b}{|A^T v|} \frac{A^T v}{|A^T v|} \quad \text{for } v \sim \tau.$$

We again have a special interest in the case $\tau = \text{Unif}(\mathbb{S}^{d-1})$, which corresponds to the *coordinate-free randomized Kaczmarz algorithm*.

Lemma 6. Let $x^* \in \mathbb{R}^m$ be the solution to (55). Starting from any initial state $x_0 \in \mathbb{R}^m$, the iterates $(x_k)_{k \geq 0}$ of the generalized randomized Kaczmarz algorithm converge to x^* in the sense that

$$\sqrt{\mathbb{E}|x_k - x^*|^2} \leq (1 - \rho)^k |x_0 - x^*| \quad \text{with rate } \rho = \frac{1}{2} \inf_{|\zeta|=1} \mathbb{E}_{v \sim \tau} \left(\zeta \cdot \frac{A^T v}{|A^T v|} \right)^2. \quad (57)$$

In the special case where the probability measure τ is given by

$$\tau = \|A\|_F^{-2} \sum_{i=1}^d |A^T e_i|^2 \delta_{e_i}$$

the generalized randomized Kaczmarz algorithm reduces to the classical randomized Kaczmarz algorithm. In this case, Lemma 6 recovers the sharp convergence rate from [36]:

$$\rho = \frac{1}{2} \|A\|_F^{-2} \inf_{|\zeta|=1} \sum_{i=1}^d |A^T e_i|^2 \left(\zeta \cdot \frac{A^T e_i}{|A^T e_i|} \right)^2 = \frac{1}{2} \|A\|_F^{-2} \inf_{|\zeta|=1} |A\zeta|^2 \geq \frac{1}{2} \|A\|_F^{-2} \|A^{-1}\|^{-2}. \quad (58)$$

Here, $\|\cdot\|_F$ denotes the Frobenius matrix norm, and $\|\cdot\|$ denotes the operator norm. The inequality in (58) follows from the fact that the left inverse A^{-1} satisfies $|z| \leq \|A^{-1}\| |Az|$ for all $z \in \mathbb{R}^m$.

Proof of Lemma 6. Let $x_0 \in \mathbb{R}^m$ and consider synchronously coupled iterations starting from x_0 and x^* :

$$x_1 = \Pi_{A^T v} x_0 + \frac{v \cdot b}{|A^T v|} \frac{A^T v}{|A^T v|} \quad \text{and} \quad x^* = \Pi_{A^T v} x^* + \frac{v \cdot b}{|A^T v|} \frac{A^T v}{|A^T v|} \quad \text{using the same } v \sim \tau.$$

Since x^* is a fixed point of the iteration,

$$x_1 - x^* = \Pi_{A^T v} (x_0 - x^*).$$

By Lemma 1, we have

$$\mathbb{E}_{v \sim \tau} |x_1 - x^*|^2 = \mathbb{E}_{v \sim \tau} |\Pi_{A^T v} (x_0 - x^*)|^2 \leq (1 - 2\rho) |x_0 - x^*|^2$$

where ρ is defined in (57). The proof is completed by iterating this bound, taking square roots, and using $\sqrt{1 - 2x} \leq 1 - x$ valid for $x \in [0, 1/2)$. \square

In certain settings, Lemma 6 implies a diffusive to ballistic speed-up for *coordinate-free randomized Kaczmarz* compared to the classical *randomized Kaczmarz*, analogous to the speed-up observed for *Hit-and-Run* compared to *random-scan Gibbs*. To illustrate, consider the bivariate example

$$A = \begin{pmatrix} 0 & 1 \\ a & 1 \end{pmatrix} \quad \text{for } a \in (0, 1) \text{ small.} \quad (59)$$

Randomized Kaczmarz, being restricted to move along the directions $(0, 1)$ and $(a, 1)$, is constrained to directions that are nearly orthogonal to e_1 . As a result, it exhibits slow convergence due to predominantly local moves along e_2 . In contrast, the coordinate-free randomized Kaczmarz algorithm moves in the direction $A^T v$ with $v \sim \text{Unif}(\mathbb{S}^1)$, enabling global moves along e_1 with sufficiently high probability, thereby accelerating convergence, see Figure 7.

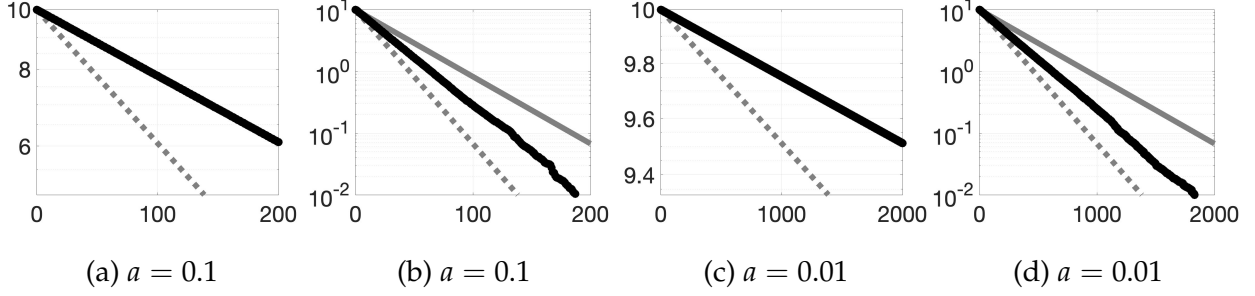


Figure 8: Convergence of randomized Kaczmarz (a), (c) vs. coordinate-free randomized Kaczmarz (b), (d) for $Ax = 0$, with A as defined in (59), starting from $x_0 = (-10, 0)$. Solid black lines show the mean error $\sqrt{\mathbb{E}|x_k - x^*|^2}$ averaged over 10,000 realizations. Only the coordinate-free variant converges within the displayed number of iterations. Solid gray lines show the theoretically guaranteed diffusive rate $a^2/4$ in (a),(c) and ballistic rate $a/4$ in (b), (d), while dotted gray lines indicate twice these theoretical rates. Randomized Kaczmarz converges exactly at the theoretical rate, while coordinate-free randomized Kaczmarz converges within an absolute constant of the theoretical rate.

For randomized Kaczmarz, the diffusive rate can be derived from (58):

$$\rho = \frac{1}{2} \|A\|_F^{-2} \inf_{|\zeta|=1} |A\zeta|^2 = \frac{a^2}{2(2+a^2)} \asymp \frac{a^2}{4}. \quad (60)$$

On the other hand, for the coordinate-free randomized Kaczmarz algorithm, the rate of convergence improves to the ballistic rate:

$$\rho = \frac{1}{2} \inf_{|\zeta|=1} \mathbb{E}_{v \sim \text{Unif}(S^1)} \left(\zeta \cdot \frac{A^T v}{|A^T v|} \right)^2 = \frac{a(1+a)}{2(2+a(2+a))} \asymp \frac{a}{4}. \quad (61)$$

This diffusive to ballistic speed-up is numerically illustrated in Figure 8.

References

- [1] H. Andersen and P. Diaconis. “Hit and run as a unifying device”. In: *J. Soc. Fr. Stat. & Rev. Stat. Appl.* 148 (Jan. 2007) (cit. on pp. 2, 3).
- [2] F. Ascolani, H. Lavenant, and G. Zanella. *Entropy contraction of the Gibbs sampler under log-concavity*. 2024. arXiv: 2410.00858 [math.PR] (cit. on p. 3).
- [3] C. Bélisle, A. Boneh, and R. J. Caron. “Convergence properties of hit-and-run samplers”. In: *Comm. Statist. Stochastic Models* 14.4 (1998), pp. 767–800 (cit. on p. 3).
- [4] N. Bou-Rabee, B. Carpenter, and M. Marsden. *GIST: Gibbs self-tuning for locally adaptive Hamiltonian Monte Carlo*. 2024. arXiv: 2404.15253 [stat.CO] (cit. on p. 3).
- [5] N. Bou-Rabee and A. Eberle. “Mixing Time Guarantees for Unadjusted Hamiltonian Monte Carlo”. In: *Bernoulli* 29.1 (2023), pp. 75–104 (cit. on p. 16).
- [6] N. Bou-Rabee and S. Oberdörster. “Mixing of Metropolis-adjusted Markov chains via couplings: The high acceptance regime”. In: *Electronic Journal of Probability* 29 (2024), pp. 1–27 (cit. on p. 16).

- [7] G. Casella and E. I. George. “Explaining the Gibbs sampler”. In: *The American Statistician* 46.3 (1992), pp. 167–174 (cit. on p. 1).
- [8] M.-F. Chen and F.-Y. Wang. “Application of coupling method to the first eigenvalue on manifold”. In: *Sci. China Ser. A* 37.1 (1994), pp. 1–14 (cit. on p. 11).
- [9] M.-H. Chen and B. Schmeiser. “Performance of the Gibbs, hit-and-run, and Metropolis samplers”. In: *J. Comput. Graph. Statist.* 2.3 (1993), pp. 251–272 (cit. on pp. 3, 4, 7).
- [10] Y. Chen and R. Eldan. *Hit-and-run mixing via localization schemes*. 2022. arXiv: [2212.00297](https://arxiv.org/abs/2212.00297) [math.PR] (cit. on pp. 3, 7).
- [11] Y. Chen and R. Eldan. “Localization schemes: A framework for proving mixing bounds for Markov chains”. In: *2022 IEEE 63rd Annual Symposium on Foundations of Computer Science (FOCS)*. IEEE. 2022, pp. 110–122 (cit. on p. 3).
- [12] P. de Valpine, D. Turek, C. Paciorek, C. Anderson-Bergman, D. Temple Lang, and R. Bodik. “Programming with models: writing statistical algorithms for general model structures with NIMBLE”. In: *Journal of Computational and Graphical Statistics* 26 (2017), pp. 403–417 (cit. on p. 1).
- [13] A. Eberle and M. B. Majka. “Quantitative contraction rates for Markov chains on general state spaces”. In: *Electronic Journal of Probability* 24.none (2019), pp. 1–36 (cit. on p. 16).
- [14] A. E. Gelfand and A. F. M. Smith. “Sampling-based approaches to calculating marginal densities”. In: *J. Amer. Statist. Assoc.* 85.410 (1990), pp. 398–409 (cit. on p. 1).
- [15] S. Geman and D. Geman. “Stochastic relaxation, Gibbs distributions, and the Bayesian restoration of images”. In: *IEEE Transactions on pattern analysis and machine intelligence* 6 (1984), pp. 721–741 (cit. on p. 1).
- [16] R. J. Glauber. “Time-dependent statistics of the Ising model”. In: *J. Mathematical Phys.* 4 (1963), pp. 294–307 (cit. on p. 1).
- [17] R. M. Gower and P. Richtárik. “Randomized iterative methods for linear systems”. In: *SIAM J. Matrix Anal. Appl.* 36.4 (2015), pp. 1660–1690 (cit. on p. 23).
- [18] R. M. Gower and P. Richtárik. *Stochastic Dual Ascent for Solving Linear Systems*. 2015. arXiv: [1512.06890](https://arxiv.org/abs/1512.06890) [math.NA] (cit. on p. 23).
- [19] A. Joulin and Y. Ollivier. “Curvature, concentration and error estimates for Markov chain Monte Carlo”. In: *Ann. Probab.* 38.6 (2010), pp. 2418–2442 (cit. on p. 10).
- [20] S. Kaczmarz. “Approximate solution of systems of linear equations”. In: *Internat. J. Control* 57.6 (1993). Translated from the German, pp. 1269–1271 (cit. on p. 23).
- [21] R. Kannan, L. Lovász, and M. Simonovits. “Random walks and an $o^*(n^5)$ volume algorithm for convex bodies”. In: *Random Structures & Algorithms* 11.1 (1997), pp. 1–50 (cit. on p. 2).
- [22] Y. Kook, S. S. Vempala, and M. S. Zhang. *In-and-Out: Algorithmic Diffusion for Sampling Convex Bodies*. 2024. arXiv: [2405.01425](https://arxiv.org/abs/2405.01425) [cs.DS] (cit. on pp. 2, 3).
- [23] L. Lovász. “Hit-and-run mixes fast”. In: *Math. Program.* 86.3 (1999), pp. 443–461 (cit. on p. 2).
- [24] L. Lovász and S. Vempala. “Fast algorithms for logconcave functions: Sampling, rounding, integration and optimization”. In: *2006 47th Annual IEEE Symposium on Foundations of Computer Science (FOCS’06)*. IEEE. 2006, pp. 57–68 (cit. on p. 2).
- [25] L. Lovász and S. Vempala. “Hit-and-run from a corner”. In: *Proceedings of the thirty-sixth annual ACM symposium on Theory of computing*. 2004, pp. 310–314 (cit. on p. 2).

- [26] N. Madras and D. Sezer. “Quantitative bounds for Markov chain convergence: Wasserstein and total variation distances”. In: *Bernoulli* 16.3 (2010), pp. 882–908 (cit. on p. 16).
- [27] P. Monmarché. “High-dimensional MCMC with a standard splitting scheme for the under-damped Langevin diffusion.” In: *Electronic Journal of Statistics* 15.2 (2021), pp. 4117–4166 (cit. on p. 16).
- [28] Y. Ollivier. “Ricci curvature of Markov chains on metric spaces”. In: *Journal of Functional Analysis* 256.3 (2009), pp. 810–864 (cit. on pp. 10, 11).
- [29] A. B. Owen. *Monte Carlo theory, methods and examples*. <https://artowen.su.domains/mc/>, 2013 (cit. on p. 1).
- [30] M. Plummer et al. “JAGS: A program for analysis of Bayesian graphical models using Gibbs sampling”. In: *Proceedings of the 3rd international workshop on distributed statistical computing*. Vol. 124. 125.10. Vienna, Austria. 2003, pp. 1–10 (cit. on p. 1).
- [31] G. Roberts and J. Rosenthal. “One-shot coupling for certain stochastic recursive sequences”. In: *Stochastic processes and their applications* 99.2 (2002), pp. 195–208 (cit. on p. 16).
- [32] G. O. Roberts and S. K. Sahu. “Updating schemes, correlation structure, blocking and parameterization for the Gibbs sampler”. In: *Journal of the Royal Statistical Society Series B: Statistical Methodology* 59.2 (1997), pp. 291–317 (cit. on p. 4).
- [33] D. Rudolf and M. Ullrich. “Comparison of hit-and-run, slice sampler and random walk metropolis”. In: *J. Appl. Probab.* 55.4 (2018), pp. 1186–1202 (cit. on p. 3).
- [34] R. L. Smith. “Efficient Monte Carlo procedures for generating points uniformly distributed over bounded regions”. In: *Oper. Res.* 32.6 (1984), pp. 1296–1308 (cit. on p. 2).
- [35] D. Spiegelhalter, A. Thomas, N. Best, and W. Gilks. “BUGS 0.5: Bayesian inference using Gibbs sampling manual (version ii)”. In: *MRC Biostatistics Unit, Institute of Public Health, Cambridge, UK* (1996), pp. 1–59 (cit. on p. 1).
- [36] T. Strohmer and R. Vershynin. “A randomized Kaczmarz algorithm with exponential convergence”. In: *J. Fourier Anal. Appl.* 15.2 (2009), pp. 262–278 (cit. on pp. 4, 5, 23, 25).
- [37] V. F. Turchin. “On the computation of multidimensional integrals according to the Monte Carlo method”. In: *Teor. Veroyatnost. i Primenen.* 16 (1971), pp. 738–743 (cit. on p. 2).
- [38] S. Vempala. “Geometric random walks: a survey”. In: *Combinatorial and computational geometry* 52.573-612 (2005), p. 2 (cit. on p. 2).